Response to reviews

We thank all reviewers for the constructive suggestions and comments. Reviewer comments are listed in red. Author responses are in plain text labeled with [R]. Specific modifications to the manuscript are in blue.

Reviewer #3 (published 19 September 2014)

The paper of Chen et al. describes…

In my opinion the significance of this paper is that different SOM production pathways can be found by using the PMF. This paper addresses relevant scientific questions, however, the main issue is that a substantial portion of the results (and conclusions) presented in this paper have already been published in Chen et al. (2009) even though the data analysis was different. Therefore my main concern regards the novelty of the paper. Overall, this paper is well written and the structure of paper is clear and easy to follow. I think this paper merits publication after addressing the issues listed below.

General comments

As mentioned above, a large part of the results and following conclusions have been published earlier. Therefore I'd suggest making a clear difference which results are novel in this paper and which ones have already been published. That would be fair to the readers.

[R0] We thank the reviewer for the valuable feedback. This paper presents a follow-up research of Chen et al. (2009), in which in-Basin sources that have been suggested as major contributors of submicron OA are segmented quantitatively. For clarification, the manuscript is carefully revised. New results are highlighted. Statements related to the results that have been published in Chen et al. (2009) are either removed or revised with proper citations. Specifically, the Introduction section (p16155, line 13-28) is revised to clarify the goal of this research and the difference between results published in Chen et al. (2009) and this study. Experimental details and results that have been provided in Chen et al. (2009) are deleted (including p16157, line 1-24; p16158, line 13-17, 21-25; p16159, line 1-2; p16164, line 4-6; p16167, line 11-25; and lines in Sect. A and Sect. B of the Supplement). Moreover, modifications are made in the Results and Discussion section (p16163, line 16-22; p.16164, line 10 to p1616, line 22) to clarify the new results vs. published ones.

Specific comments

1. Abstract: page 16153, line 7; "Ammonium was present in sufficient quantities to partially neutralize sulfate". Later it was said that: "there was insufficient ammonium to neutralize sulfate" (page 16161). I understand that the meaning is same but I prefer using the latter for clarity.

[R1] This sentence is revised as suggested.

2. Abstract and throughout the manuscript; make sure that when the abbreviations are used for the first time, you also write the whole definition e.g. HOA and OOA in abstract, IEPOX, MVK and MACR in results and discussion.

[R2] Changes are made to make sure that abbreviations are defined in parentheses the first time they are used.

3. Site and instrument description: page 16157, lines 25- ; PMF was conducted on medium-resolution V-mode data but reported in unit mass resolution. Why?

[R3] The resolution of V-mode AMS data is about 2000. The data are typically analyzed in two ways. In one way, the signals are summed for each m/z window. Although there might be multiple peaks in one window, data are reported in unit mass resolution (UMR). Alternatively, the ion signals can be determined by multi-peak fitting (i.e., called high-resolution data). However, such non-linear fitting process may increase the noise level for low signals. For cases like Amazon having very low OA concentrations, the PMF analysis on the high-resolution data show similar four factors compared to the analysis on the UMR data, but worse separation for HOA. That's because although more ions are quantified in the high-resolution data, many of them have signal-to-noise ratios lower than the corresponding UMR fragments. We therefore decided to only report in UMR.

4. Results and discussion; I suggest keeping the discussion on inorganic species as short as possible as the title of the paper is "Fine mode organic mass concentrations. . .". Only if they are relevant to organics they should be discussed.

[R4] We think the information about inorganic species are important because this is the first on-line measurements of the chemical composition of submicron particles in Amazon and measurements are challenging, and the majority of this part has not been published in Chen et al. (2009). We have revised the title to match with the content. The new title is "Submicron Particle Mass Concentrations and Sources in the Amazonian Wet Season". Redundant discussions that have been covered in Chen et al. (2009) are deleted in the revised manuscript.

5. Results and discussion: page 16163, lines 26-28; you said that species correlated but R2 values were 0.35-0.52. To me these were only moderate correlations.

[R5] We agree with the reviewer that the R^2 values are not high. The purpose was to show the correlations of OOA-1 with those tracers are better than other factors with them. We have revised this part as "The correlations of the statistical loadings of the OOA-1 factor with the measured mass concentrations of biomass burning tracers, such as chloride (R^2 = 0.52), potassium (R^2 = 0.35), and black carbon (R^2 = 0.43) in the submicron particle population, were not high, possibly because of the mixing of sources to these tracers such as primary biological particles (i.e., contributing chloride and potassium) and regional pollution from Manaus to (i.e., black carbon). These correlation value were, however, significantly greater than those of the other three factors (HOA, OOA2, and OOA-3) with the tracers (i.e., $R^2 < 0.10$ for chloride, $R^2 < 0.02$ for potassium, and $R^2 < 0.20$ for black carbon) (Fig. 6b)".

6. Results and discussion, page 16166, lines 27- ; you talk about the different fractional contributions of OOA-2 and OOA-3 during different periods. Have you found any reasons why the fractions differed so much?

[R6] The weather conditions were different for the two periods. It was sunny and warmer with occasional clouds during the first period but rainy and cooler during the second period, which possibly drove the difference in the mass fraction of PMF factors. We have added the discussion of the meteorological conditions as follows: "Figure 9 shows that the relative importance of each process as a contributor differed with time and highlights two focus periods. Precipitation and temperature were the major meteorological factors that differed between the two periods. The first period was sunny, warmer with occasional clouds, and the second period had frequent heavy rainfall events. Long-range back-trajectory analyses presented in Martin et al. (2010b) showed that the air masses consistently arrived from the equatorial Atlantic Ocean passing as northeasterlies through the Amazon basin. Local measurements showed that the daytime winds mainly came from the north and northeast (Fig. 9, top)… Figure 9 shows that the loading fraction of the OOA-2 factor consistently dropped following heavy rainfall events, suggesting more efficient in-cloud or below-cloud scavenging for the types of material represented by OOA-2 than for those types represented by OOA-3. This finding further supports the interpretation that the OOA-2 factor represents, at least in part, aqueous-phase production pathways because SOM produced in this way has greater water solubility and hence greater wet deposition rates than SOM produced freshly by gas-to-particle condensation, as interpreted for the OOA-3 factor. Figure 9 also shows that the mode diameter of organic material in period 1, which has a higher OOA-2 loading fraction, is significantly larger than that in period 2, which has a higher OOA-3 loading fraction. Aqueous-phase processing is anticipated to add additional organic material that results in larger mode diameters after dehydration."

7. Results and discussion; I guess you also measured particle size distributions with the AMS. Could you get any support for the PMF factors from the pToF data?

[R7] Yes, we measured particle size distributions. The data are however very noisy because of the low concentrations. We are unable to derive the statistic size distributions for the PMF factors. When comparing the two case periods (i.e., the period having dominant contribution of OOA-2 and the period mainly contributed by OOA-3, we found the mode-diameter for OOA-2 was greater than that for OOA-3, which is consistent with our interpretation of OOA-2 from sustained particle-phase pathways although not conclusive. We have modified Fig. 9 with this addition and modified the related discussions (please see R6 for more details).

8. Conclusions; This section is mostly summarizing the results. Only the last paragraph concludes. Maybe the title should be summary and conclusions?

[R8] We have revised this section with the focus of the last paragraph.

9. Figure 5, page 16182; Figure is a bit unclear. I suggest using dots only to PMF factors and lines to all the other components, or something similar.

[R9] We thank the reviewer for the suggestion and have updated the figure.

Reviewer #4 (published 6 November 2014)

The study presents new information of chemical composition of organic aerosols in the Amazon. The results are important and interesting, especially since there are few previous studies in this environment.

My main concern is that the results in some parts seem to be over-interpreted, and some conclusions are not well-supported by the data analysis. This regards the interpretation of the PMF factors OOA-2 and OOA-3, which only differ slightly in average mass spectrum and time variation. The associated uncertainty should be better reflected in the abstract, discussion and conclusions. OOA-2 is "implicated as associated with reactive uptake of isoprene products... to haze, fog or cloud droplets", while OOA-3 is "consistent with fresh production SOM by a mechanism of gas-phase oxidation of BVOC followed by gas-to-particle conversion of the oxidation products" (from abstract). These strong statements should be modified to better reflect the data, uncertainty and analysis.

[R10] We thank reviewer #4 for the valuable feedback. We have carefully revised the results and discussion section, particularly on the interpretation of OOA-2 and OOA-3. Detailed comparisons between the mass spectra of the PMF factors and the spectra of chamber SOM are made. Additional information from literature and the analysis of meteorological conditions is added to support conclusions. Statements are rephrased based on the associated uncertainties. Detailed responses to the individual comments are given below.

The supplemental material is quite extensive. 34 pages supplement to an 18 page manuscript seem like too much for a journal like ACP. I suggest moving some of the most important sections and figures to the main text.

[R11] We have moved section D and Figure S9 to the main text. Also redundant details in Sect. A of the Supplement that have been provided in Chen et al. (2009) are deleted.

The results and discussion section should include at least some information on meteorology (boundary layer heights and wind patterns) at the site, especially in the discussion of time series and daily patterns.

[R12] We have added some information on the boundary layer, local wind, back trajectories, and weather conditions to support our discussion of PMF factors. Please see R6 and Fig. 9 for more details. More detailed information on meteorology is provided in the overview paper by Martin et al. (2010).

Previous studies in the Amazon have observed primary biological aerosols – were there any indications of primary biological aerosols in the present data?

[R13] The PMF analysis conducted herein does not suggest a factor for primary biological aerosol particles (PBAP). Possible reasons include (1) the marker ions are not unique and have contributions from other sources (e.g., secondary organic material), (2) the concentration level is low so that the PMF analysis only extracted information from the UMR data (see R3), and (3) the contribution of PBAP to the submicron organic aerosol mass is small. Schneider et al. (2011)

semi-quantified the primary biological aerosols during AMAZE-08 by using mass spectral markers and placed an upper limit of 20% to their mass contributions to submicron organic aerosols. This information is now provided in Introduction.

Specific comments:
Page 16154 line 15: Oxidation of BVOC correlates with other factors beside sunlight – please be more specific.

[R14] This sentence is revised.

Page 16157 line 5-8: The statement on density seems misplaced here.

[R15] Since the calculation of density is discussed in the Supplement, we have deleted these lines in the main text.

p. 16158 and supplement: The authors spend quite some time to discuss that they do not observe organosulfates in their data. The sulfate levels are quite low, and since organosulfates are only expected to constitute a fraction of this, their concentrations should be very low. What is the detection limit for organosulfates using AMS?

[R16] The molecular weight of organosulfates is much greater than sulfate. If a substantial fraction of the detected sulfate is from organosulfates, the concentration of organosulfates might not be low. Some studies suggest a large contribution of organosulfate to the organic mass concentration, especially for acidic particles (Surratt et al., 2008; Iinuma et al., 2009). During AMAZE-08, submicron particles are acidic. Therefore, it is important to evaluate the potential contribution of organosulfates. The AMS detection limit for organosulfates is estimated to be ~0.06 μg m^{-3} given a detection limit of sulfate of 0.02 μg m^{-3} and an assumed molecular weight of organosulfates of 300 g mol^{-1}.

P. 16160 L4: Would biomass burning in Africa give a covariance of BC with sulfate at your site?

[R17] Studies have shown that sulfate and BC in the fine mode were both elevated during long-range transport events in the central Amazon (Martin et al., 2010b and references therein). Based on satellite, lidar, and back-trajectory analysis, we concluded that the particles during AMAZE-08 were affected at times by dust transport from northern Africa and biomass burning in equatorial Africa.

P16161 L17-22: The argument is not clear here. First you say that the charges nearly balanced and then you state the relative proportions within each group, which does not provide information on the degree of charge balance. In several places you mention that the aerosols were acidic. How did you arrive at that conclusion based on your data?

[R18] The charges were nearly balanced when looking at the fine mode (PM_2) data obtained by IC. For the submicron domain, we integrated information of the concentrations of non-refractory species detected by AMS, concentrations of other cations obtained from PM_2-IC data (for the entire campaign) and the size distributions of these cations obtained from MOUDI-IC data (one

sample for AMAZE-08 as well as Fig. 9c in Fuzzi et al. (2007)). The results indicated that the particles were acidic and probably presented as bisulfate. For clarification, we have deleted p16161, L16-22 and added the following statement in L12: "The AMS is unable to quantify refractory components such as K+, Na+, Ca2+, and Mg2+. Mass-diameter distributions of these ions obtained by IC analysis of samples collected by a Multi-Orifice Uniform Deposit Impactor (MOUDI) on 22 March 2008 suggest that 40% of the mass of these ions was distributed to the submicron particle fraction. For comparison, Fuzzi et al. (2007) for the wet season reported 50-60% of K+ and Ca2+ in the submicron fraction, compared to the predominance of Na+ and Mg2+ in the supermicron fraction. The campaign-average fine-mode mass concentrations of K+, Ca2+, Na+, and Mg2+ measured by IC were 0.03, 0.01, 0.02, and 0.01 μg m 3, respectively. The implication of the relative concentrations (i.e., sulfate concentration of 0.19 ± 0.06 μg m-3) is that the submicron inorganic ion composition is reasonably approximated as ammonium bisulfate during AMAZE-08.".

P16161 L. 8-11: statements 1) and 2) seem somewhat redundant.

[R19] The statement of "(i.e., requiring a molar ratio of 2)" is removed.

P. 16163 L26: The correlations are not very strong, probably due to a mix of sources for the tracers. A term like "correlated somewhat" would describe this better.

[R20] We agree with the reviewer. This statement is revised. Please see R5 for more details.

P. 16164 L. 11: The peak at m/z 82 is not prominent in Fig. 4c. I agree that is present and visible, but it is far from being prominent. Furthermore the relative intensities of m/z 53 and 55 in OOA-2 and OOA-3 are too similar to state that 53 is "elevated". The text should better reflect the data here.

[R21] We have gone through the manuscript. Similar descriptions are rephrased (e.g., "characteristic peak".

P. 16164 L25: What is number of observations included in calculation of the correlation coefficient? How many days did the correlation include?

[R22] About seven days including ~1000 observations.

P. 16164 L27-29: Should be rewritten to reflect that your OOA-2 factor somewhat resemble the spectra of Budisulistiorini et al, not the other way around.

[R23] We meant the IEPOX-OA factor reported in Budisulistiorini et al. (2013) not our OOA-2 factor in this sentence. For clarification, we have revised this paragraph by specifying the factor name used in the references such as "… Borneo (named as the "82Fac" factor) …Ontario, Canada (named as the "UNKN" factor) … Atlanta, Georgia, USA (named as the "IEPOX-OA" factor) … "OOA-2" of this study and "82Fac", "UNKN", and "IEPOX-OA" of earlier studies".

P16165 L1: Unless the reference Kuwata et al., has been updated, the statement

should be removed, since it does not add to the readers understanding of the present work.

[R24] We have replaced Kuwata et al. by Liu et al. (2014) which is from the same study and is already published.

P16165 L5: How did you measure/calculate that the particles were acidic? How acidic were they?

[R25] Please see R18 for the answers.

P16165 L7-22: The paragraph is quite speculative and ends with a conclusion that OOA-2 represents both degree of emission and oxidation of isoprene, as well as uptake of these products in particles, in addition to uptake and aqueous phase processes involving other precursors. It would be nice if the latter part could be supported by data or more precise references. I agree that these are possible explanations for the factor, but it is important that the text (here, as well as in the conclusion and abstract) reflects the associated uncertainty.

[R26] We have carefully revised the discussion in p16164-16165. Results from a recent publication (Liu et al., 2014) are cited to support the discussion. Detailed comparisons between the mass spectra of the OOA-2 factor and the spectra of chamber IEPOX or isoprene SOA are made. Possible explanations (not just aqueous-phase processing) are listed.

P16165 L23-: The figure (4d) does not support the statement that m/z 55 and 91 are "distinct".

[R27] The statement is changed to be "The OOA-3 factor had a prominent peak at *m*/*z* 43. For *m*/*z* > 80, the most intense peak occurred at *m*/*z* 91".

P16166 L1-2: "a linear combination of the three chamber spectra largely reproduced the OOA-3 factor". The ion of highest intensity m/z 29 is not well modeled with the chamber spectra – why?

[R28] One reason is that our chamber isoprene SOM likely formed from both gas-to-particle condensation and reactive-uptake of IEPOX pathways. The spectra of laboratory IEPOX SOM also show high intensity at *m*/*z* 29 (Budisulistiorini et al., 2013; Liu et al., 2014). We added this discussion in the revised manuscript.

P16166 L 10-11: For how many days did OOA-3 track the BVOC concentrations?

[R29] About 6 days.

P16167 L18: "the OOA-2 factor was consistent with the reactive uptake of isoprene oxidation products". Consistent is a very strong word here. It is more fair to say that it showed similarities or it was interpreted as uptake isoprene oxidation products on aerosol particles.

[R30] We have gone through the manuscript and rephrased such statements.

P16166 L22-24. Was there changes in the boundary layer height during the day?

[R31] The boundary layer height was 50-100 m at night and increased to 700-800 m by local noon time. This information is added to the main text.

Figure 6: The legends should be more clearly described in the figure text. What is "the OH family"? It is very interesting that these experiments have been performed at different concentrations. The results show the variation in the relative intensities, and thus give information on the uncertainty in these studies.

[R32] This figure has been updated. The legend information is added to the figure caption. We also changed "OH family" to be "$H_yO_1^+$ family" for clarification.

Supplement
Please check that the references to figures and tables are in chronological order.

[R33] We checked the order and changes are made.

P5: Please update and add the reference Canagaratna et al. 2013. "The contributions of organonitrates and organosulfates, detected as inorganic nitrate or sulfate ions, to the elemental ratios were negligible because their low mass concentrations." The statement should have a reference to the discussion later in the Appendix.

[R34] The reference is updated to "Canagaratna et al. (2015)". The statement that the reviewer pointed out has been revised as a separate paragraph that provides quantitative discussion on the concentrations of organosulfate and organonitrate species. Previous description about organosulfate (also in sect. A of the supplement) and organonitrate (in main text, p16159 Line 14-20) are combined to this new paragraph.

P6: "The two types of filters show reasonable agreement". The statement should be further elaborated or at least give a reference to data in the manuscript or published papers.

[R35] The statement is changed to be "The two types of filters show reasonable agreement on the particle mass concentration (Table S2)."

P12: "The prominent C7H7+ companied with a negligible signal of C6H13+ at m/z 85 is also unique for the three biogenic SOA studied in the chamber". The reader cannot judge the statement since only data for BSOA is given. Give at least a reference here. The last sentence of "prominent" m/z 82 should be corrected as discussed above. I suggest to move section D to the main manuscript. Furthermore, I suggest that Figure S9 is included in the main manuscript.

[R36] We have moved Sect. D and Fig. S9 to the main text. The descriptions of the mass spectra are carefully revised. Comparisons to the spectra of other types of organic aerosol from the literature with references are made.

Please extend the figure texts for figures S12-S14, so the reader is able to understand them without reading the full text.

[R37] This change is made.

Reviewer #5 (published 10 November 2014)

General comments
This paper presents the results of on-line measurements of sub-micrometer organic aerosol (OA) obtained in a tropical rainforest in the Amazon during the wet season. The study examines in detail the formation pathways for OA, by mainly focusing on statistical analysis (i.e., PMF) of the HR-ToF-AMS data sets. Based on these analysis, the authors suggest the comparable importance of particle-phase and gas-phase pathways for the secondary production of OA during the study period.

The present work may provide valuable data in our understanding on formation processes of OAs particularly associated with the oxidation of biogenic VOCs. The manuscript fits with the scientific scope of ACP. In my opinion, however, new scientific finding does not seem to be emphasized in comparison with some previous works. Although a data set presented is valuable, there are some important issues that need to be worked out. I recommend its publication in ACP after some revisions raised below.

[R38] We thank the reviewer for the valuable feedback. We have carefully revised the manuscript to highlight our new findings. Please see R0 for more details.

Specific comments
(1) My major concern is about the discussion on Figure 8: What is the major difference between the Period 1 and Period 2 from viewpoints of meteorological conditions, photochemical field, etc.? What is the major factor controlling the fractional contributions by each factor, particularly OOA-2 and OOA-3? None of the explanation has been made in the text. The authors should discuss these points because this is one of the most important part of this paper.

[R39] Yes, we have added the discussion on the meteorological conditions for the two focus periods. We think that the precipitation is one driven factor of different fractional contributions of OOA-2 and OOA-3. Please see R6 and Fig. 9 for more details.

(2) Figure 9 summarizes the processes for BSOA in the Amazonian wet season. However, most of the processes shown in the figure have been already reported or suggested in previous studies and seem to be somewhat "general" picture which one can find in a textbook. The authors should

emphasize in the figure what the new findings are in this study with making a quantitative statement.

[R40] The caveat is that multivariate statistical factors do not correspond to segregated individual chemical components (e.g., unlike molecules or families of molecules), although the factors can be indicative of the relative importance of different atmospheric emissions and pathways. Given this caveat in mind and the fact that the main text is already quite extensive after taking other reviewer's suggestions, we decided to remove Fig. 9 in the main text.

(3) If the OOA-2 factor represents the particle-phase reactions, then what is the time scale for this factor? The reaction is expected to be much faster than that represented by the OOA-3 factor which is associated with gas-to-particle partitioning of the BVOC oxidation products on a timescale of several hours (P. 16166, L7-9). Are these timescales supported by the time lag between OOA and BVOC? It is not clear from the diurnal profiles in Figure 7.

[R41] We agree with the reviewer that the reactive uptake of IEPOX isomers is probably rapid. The gas-to-particle condensation is also considered to be spontaneous. The formation of OOA-2 and OOA-3 is therefore regulated by the timescale of the production of gas-phase products by BVOC photochemistry. The diel profiles of OOA-2 and OOA-3 both peak in the earlier afternoon as is consistent with photochemically driven production. It is however difficult to quantify the time lag (if any) between OOA and BVOC based on the diel profiles because these profiles were influenced by local precipitation (e.g., Fig. S7). By looking at the time series (Fig. 6), there may be 1-2 h lag between OOA and BVOC (e.g., on 13 Feb and 17 Feb). The data coverage is however limited. We are unable to draw a quantitative conclusion on these timescales.

(4) P.16163, L.16-18: "The OOA-1 factor… African biomass burning." I cannot logically understand this sentence. Do the sentences below in this paragraph (P.16163, L.18-P.16164, L.9) support this sentence?

[R42] Yes, later sentences provide support. We have removed revised this sentence as "The OOA-1 factor had the feature of a singularly dominant peak at *m*/*z* 44 (Fig. 5b), which has been linked to organic material that has undergone extensive oxidation during a prolonged atmospheric residence time (~10 days)". The statement of "was believed to be mainly associated with long-range transport of African biomass burning" is removed since it has been address in the later text.

(5) P.16163, L.19: "a prolonged atmospheric residence time" What is the exact time scale for this? Please provide more quantitative statement.

[R43] We meant a time scale of "~10 days", which has been added to this statement.

(6) P.16163, L.27: Chloride is also a tracer for sea salt, and black carbon can be attributed to not only the biomass burning emissions, but also other burning sources, such as fossil fuel burning. The authors should rephrase the sentence or change the logic of it.

[R44] We have rephrased the sentence. Please see R5 for more details.

(7) P.16163, L.23: “Africa” should be “African”.

[R45] This change is made in the revised manuscript.

References

Budisulistiorini, S. H., Canagaratna, M. R., Croteau, P. L., Marth, W. J., Baumann, K., Edgerton, E. S., Shaw, S. L., Knipping, E. M., Worsnop, D. R., Jayne, J. T., Gold, A., and Surratt, J. D.: Real-time continuous characterization of secondary organic aerosol derived from isoprene epoxydiols in downtown Atlanta, Georgia, using the Aerodyne aerosol chemical speciation monitor, Environ. Sci. Technol., 47, 5686-5694, 10.1021/es400023n, 2013.

Canagaratna, M. R., Jimenez, J. L., Kroll, J. H., Chen, Q., Kessler, S. H., Massoli, P., Hildebrandt Ruiz, L., Fortner, E., Williams, L. R., Wilson, K. R., Surratt, J. D., Donahue, N. M., Jayne, J. T., and Worsnop, D. R.: Elemental ratio measurements of organic compounds using aerosol mass spectrometry: characterization, improved calibration, and implications, Atmos. Chem. Phys., 15, 253-272, 10.5194/acp-15-253-2015, 2015.

Fuzzi, S., Decesari, S., Facchini, M. C., Cavalli, F., Emblico, L., Mircea, M., Andreae, M. O., Trebs, I., Hoffer, A., Guyon, P., Artaxo, P., Rizzo, L. V., Lara, L. L., Pauliquevis, T., Maenhaut, W., Raes, N., Chi, X. G., Mayol-Bracero, O. L., Soto-Garcia, L. L., Claeys, M., Kourtchev, I., Rissler, J., Swietlicki, E., Tagliavini, E., Schkolnik, G., Falkovich, A. H., Rudich, Y., Fisch, G., and Gatti, L. V.: Overview of the inorganic and organic composition of size-segregated aerosol in Rondonia, Brazil, from the biomass-burning period to the onset of the wet season, J. Geophys. Res., 112, D01201, 10.1029/2005JD006741, 2007.

Iinuma, Y., Boge, O., Kahnt, A., and Herrmann, H.: Laboratory chamber studies on the formation of organosulfates from reactive uptake of monoterpene oxides, Phys. Chem. Chem. Phys., 11, 7985-7997, 10.1039/b904025k, 2009.

Liu, Y., Kuwata, M., Strick, B. F., Geiger, F. M., Thomson, R. J., McKinney, K. A., and Martin, S. T.: Uptake of epoxydiol isomers accounts for half of the particle-phase material produced from isoprene photooxidation via the HO2 pathway, Environ. Sci. Technol., 49, 250-258, 10.1021/es5034298, 2014.

Martin, S. T., Andreae, M. O., Artaxo, P., Baumgardner, D., Chen, Q., Goldstein, A. H., Guenther, A., Heald, C. L., Mayol-Bracero, O. L., McMurry, P. H., Pauliquevis, T., Poschl, U., Prather, K. A., Roberts, G. C., Saleska, S. R., Dias, M. A. S., Spracklen, D. V., Swietlicki, E., and Trebs, I.: Sources and properties of amazonian aerosol particles, Reviews of Geophysics, 48, Rg2002, 10.1029/2008rg000280, 2010.

Schneider, J., Freutel, F., Zorn, S. R., Chen, Q., Farmer, D. K., Jimenez, J. L., Martin, S. T., Artaxo, P., Wiedensohler, A., and Borrmann, S.: Mass- spectrometric identification of primary

biological particle markers and application to pristine submicron aerosol measurements in Amazonia, Atmos. Chem. Phys., 11, 11415-11429, 10.5194/acp-11-11415-2011, 2011.

Surratt, J. D., Gomez-Gonzalez, Y., Chan, A. W. H., Vermeylen, R., Shahgholi, M., Kleindienst, T. E., Edney, E. O., Offenberg, J. H., Lewandowski, M., Jaoui, M., Maenhaut, W., Claeys, M., Flagan, R. C., and Seinfeld, J. H.: Organosulfate formation in biogenic secondary organic aerosol, J. Phys. Chem. A, 112, 8345-8378, 10.1021/jp802310p, 2008.

~~Fine Mode Organic~~ Submicron Particle Mass Concentrations and Sources in the Amazonian Wet Season (AMAZE-08)

Q. Chen[1,*], D. K. Farmer[2,**], L. V. Rizzo[3,***], T. Pauliquevis[***], M. Kuwata[1,****], T. G. Karl[3,*****], A. Guenther[3,******], J. D. Allan[4], H. Coe[4], M. O. Andreae[5], U. Pöschl[5], J. L. Jimenez[2], P. Artaxo[6], S. T. Martin[1]

(1) School of Engineering and Applied Sciences & Department of Earth and Planetary Sciences, Harvard University, Cambridge, MA, USA
(2) Department of Chemistry and Biochemistry & Cooperative Institute for Research in Environmental Science, University of Colorado, Boulder, CO, USA
(3) National Center for Atmospheric Research, Boulder, CO, USA
(4) National Centre for Atmospheric Science & School of Earth, Atmospheric and Environmental Sciences, University of Manchester, Manchester, UK
(5) Max Planck Institute for Chemistry, Mainz, Germany
(6) Applied Physics Department & Atmospheric Science Department, University of São Paulo, São Paulo, Brazil

[*]Now at ~~Department~~State Key Joint Laboratory of ~~Civil and~~ Environmental Simulation and Pollution Control, College of Environmental Sciences and Engineering, ~~Massachusetts Institute of Technology, Cambridge, MA, USA~~Peking University, Beijing, 100871, China

[**]Now at Department of Chemistry, Colorado State University, Fort Collins, CO, USA

[***]Now at Department of Exact and Earth Sciences, Federal University of São Paulo, Diadema, Brazil

[****] Now at Nanyang Technological University and Earth Observatory of Singapore, Singapore

[*****]Now at Institute of Meteorology and Geophysics, University of Innsbruck, Austria

[******]Now at Atmospheric Sciences and Global Change Division, Pacific Northwest National Laboratory, Richland, WA, USA.

Manuscript submitted to *Atmospheric Chemistry and Physics*

Correspondence to: S.T. Martin (scot_martin@harvard.edu) and P. Artaxo (artaxo@if.usp.br)

Abstract

Real-time mass spectra of the non-refractory species in submicron aerosol particles were recorded in a tropical rainforest in the central Amazon basin during the wet season from February to March 2008, as a part of the Amazonian Aerosol Characterization Experiment (AMAZE-08). Organic material accounted on average for more than 80% of the non-refractory submicron particle mass concentrations during the period of measurements. ~~Ammonium~~There was ~~present in sufficient quantities~~insufficient ammonium to ~~partially~~ neutralize sulfate. In this acidic, isoprene-rich, HO_2-dominant environment positive-matrix factorization ~~(PMF)~~ of the time series of particle mass spectra identified four statistical factors to account for the 99% variance of the signal intensities of the organic constituents~~: an HOA~~. The first factor ~~having a hydrocarbon-like signature and~~was identified as associated with regional and local pollution~~, an OOA-1~~ and labeled as "HOA" for its hydrocarbon-like characteristics. A second factor was associated with long-range transport~~, an OOA-2~~ and labeled as "OOA-1" for its oxygenated characteristics. A third factor, labeled "OOA-2," was implicated as associated with the reactive uptake of isoprene oxidation products, especially of epoxydiols to acidic haze, fog or cloud droplets~~, and an OOA-3~~. A fourth factor, labeled as "OOA-3," was consistent with an association to the fresh production of secondary organic material (SOM) by a mechanism of gas-phase oxidation of biogenic volatile organic ~~compounds (BVOC)~~precursors followed by gas-to-particle conversion of the oxidation products. The ~~OOA~~ suffixes 1, ~~-~~2, and ~~-~~3 ~~factors had progressively less oxidized signatures. Aqueous~~on the OOA labels signify ordinal ranking with respect to the extent of oxidation represented by the factor. The process of aqueous-phase oxidation of water-soluble products of gas-phase photochemistry might also have been ~~also involved in the formation of~~associated to some extent with the OOA-2 factor. The campaign-average ~~mass~~

~~concentrations~~factor loadings were in a ratio of ~~7:5~~1.4:1 for ~~the~~ OOA-2 ~~compared to the~~ :OOA-3 ~~pathway~~, suggesting the comparable importance of particle-phase compared to gas-phase pathways for the production of SOM during the study period.

1. Introduction

Aerosol particles in the atmosphere make an important contribution to the Earth's radiation budget (IPCC, 2013). They can directly scatter and absorb shortwave and longwave radiation, and they can indirectly affect radiative forcing and precipitation by modifying cloud properties. The assessment of the impact of human perturbations on climate requires an understanding of the natural functioning of the aerosol-cloud-climate system. During the wet season, the pristine Amazon basin provides a unique environment for studying the sources and atmospheric evolution of natural aerosol particles and hence understanding the role of aerosol particles in biosphere-atmosphere interactions (Andreae, 2007; Martin et al., 2010a).

Tropical forest emissions and long-range transport from outside of the basin are major contributors to the number and mass budgets of Amazonian aerosol particles during the wet season because regional biomass burning emission is largely suppressed by heavy rainfall (Martin et al., 2010a). The forest ecosystem emits biogenic volatile organic compounds (BVOC) that can be oxidized in the atmosphere, principally by reaction with photochemically produced hydroxyl radical and ozone molecules. Some of the oxidized products have sufficiently low vapor ~~pressure to condense and form secondary organic material (SOM) in the particle phase. The oxidation of BVOC correlates with available sunlight, resulting in daytime increases in the particle-phase mass concentrations of typical BVOC-oxidation products, such as dicarboxylic acids (Graham et al., 2003a). In particular for Amazonia where the emission of the BVOC is dominated by isoprene, the concentrations of isoprene oxidation tracers (e.g., 2-methyltetrols and C_5-alkene triols) increase in the particle phase (Claeys et al., 2004, 2010)~~pressures to condense and produce SOM in the particle phase. Moreover, in haze, fog, and cloud droplets, the production of organic acids and oligomers can occur from the OH-initiated aqueous-phase

oxidation of the photooxidation products of isoprene, e.g., glyoxal, methacrolein (MACR), and methylvinyl ketone (MVK) (Lim et al., 2010), as well as from the acid-catalyzed reactive uptake of epoxydiol isomers (IEPOX) (Surratt et al., 2010; Lin et al., 2012). For SOM produced by these aqueous-phase pathways, a fraction of the mass can remain in the particle phase after dehumidification. In addition ~~to the biogenic SOM~~, the forest ~~can~~ also directly ~~emit~~emits primary biological particles containing potassium, phosphorus, sugars, sugar alcohols, and fatty acids~~.~~, including an upper limit of a 20% contribution to the submicron organic mass concentration (Graham et al., 2003a; Elbert et al., 2007; Schneider et al., 2011; Pöhlker et al., 2012). The forest also emits gases important to the particle mass concentrations of inorganic ions. For example, ammonia partitions ~~Ammonia can partition~~ from the gas phase to acidic particles (Trebs et al., 2005). Reduced sulfur gases undergo atmospheric oxidation to produces sulfuric acid that condenses to the particle phase (Andreae et al., 1990).

The Amazonian Aerosol Characterization Experiment 2008 (AMAZE-08) investigated the sources and properties of Amazonian particles (Martin et al., 2010b). Evidence from AMAZE-08 led to the conclusion that there ~~was~~is a large-scale contribution of biogenic SOM to the mass concentration of submicron aerosol particles ~~(up to 90%), at least~~ during the wet season (Chen et al., 2009; Martin et al., 2010b; Pöschl et al., 2010; Schneider et al., 2011). In particular, Chen et al. (2009) demonstrated that on order of 90% of the organic material of submicron Amazonian particles arises from the in-Basin production of biogenic SOM. Primary biogenic particles enriched in potassium salts ~~in the submicron size range were suggested~~and emitted by fungal spores as ~~seed~~10 to 20 nm dried particles ~~that provided~~possibly provide surfaces for the condensation of SOM from the gas phase (Pöhlker et al., 2012). These bio-related particles ~~participated~~participate in the regulation of the hydrological cycle of the forest by serving as

nuclei for cloud formation and subsequent precipitation (Gunthe et al., 2009; Prenni et al., 2009). In addition to particle production tied to the forest ecosystem, lidar and satellite observations ~~provided~~provide evidence of episodic long-range advection of African smoke and Saharan dust ~~(Baars et al., 2011).~~(Ben-Ami et al., 2010; Baars et al., 2011). These intrusions ~~were~~are temporally consistent with increases of heavily oxidized organic particles ~~(Chen et al., 2009)~~observed by Chen et al. (2009), indicative of long atmospheric residence times, as well as increases in the concentrations of ice nuclei ~~(Prenni et al., 2009)~~observed by Prenni et al. (2009).

~~Condensational growth has been reported as an important pathway of biogenic SOM production in Amazonia (Graham et al., 2003a; Chen et al., 2009). Pöhlker et al. (2012) further proposed a significant role of liquid-phase processing for Amazonian aerosol particles. Laboratory studies have demonstrated the production of organic acids and oligomers from the OH-initiated aqueous-phase oxidation of the photooxidation products of isoprene, e.g., glyoxal, methacrolein (MACR), and methylvinyl ketone (MVK) (Lim et al., 2010), as well as the acid-catalyzed reactive uptake of isoprene epoxydiol (IEPOX) isomers produced by the photooxidation of isoprene under HO_2-dominant conditions (Surratt et al., 2010; Lin et al., 2012). HO_2-dominant conditions refer to the fate of peroxy radicals with respect to reaction with HO_2 or NO. For SOM produced by these particle-phase pathways, a fraction of the mass may remain in the particle phase after dehumidification. The relative importance to SOM mass concentration of such particle-phase reaction pathways compared to gas-phase oxidation followed by condensation is, however, still poorly understood (Martin et al., 2010a; Ervens et al., 2011). Field characterization is crucial for constraining the relative importance of different reaction pathways.~~

The present study analyzes multiple data sets collected during AMAZE-08 in relation to

one another and in the context of the chemistry and properties of submicron particles in the Amazon basin during the wet season. ~~Positive~~A focus topic is the relative importance of aqueous-phase reactions compared to gas-phase oxidation followed by condensation to the production of SOM mass concentration. The relative importance of these two pathways remains poorly understood (Martin et al., 2010a; Ervens et al., 2011). On the one hand, condensational growth has been reported as an important pathway of the biogenic SOM production (Graham et al., 2003a). On the other hand, a significant role of liquid-phase processing for Amazonian aerosol particles is proposed (Pöhlker et al., 2012). In the current study, positive-matrix factorization of the time series of particle mass spectra is used to identify statistical factors that differ in mass spectral patterns (Zhang et al., 2011). The properties of these factors, in conjunction with the auxiliary data sets, are used to investigate the relative importance of different possible sources of ~~fine mode~~submicron organic ~~mass concentration~~material in Amazonia during the wet season.

2. Site and Instrument Description

Ground-based measurements were carried out at a rainforest site during the wet season from 7 February to 13 March 2008 (Martin et al., 2010b). The site (02 °35.68 ´S, 60 °12.56 ´W, 110 m above sea level) located 60 km NNW of Manaus and faced 1600 km of nearly pristine forest to the east to the Atlantic Ocean. The site was accessed by a 34-km unpaved road from Highway 174 (Fig. S1). The ten-day back trajectories indicated that during the measurement period the air masses mainly originated from the northeast over the Atlantic Ocean in the direction of Cape Verde and the Canary Islands. Air was sampled at the top of a tower ("TT34"; 38.75 m) above the forest canopy (33 m). Instrumentation deployed during AMAZE-08 is described in Martin et al. (2010b) ~~and Sect. A and B of the Supplement~~.

The present study focuses mostly on the statistical analysis of the data sets of an Aerodyne high-resolution Aerosol Mass Spectrometer (HR-AMS) in the context of complementary data sets of other instruments. ~~Several non-standard aspects of the AMS analysis are summarized here in the main text.~~ Mass concentrations were adjusted to standard temperature and pressure (noted as STP; 273.15 K and 10^5 Pa)~~. Additional details~~, which were approximately 10% greater than those at calibration conditions (299.3 K and 100591.7 Pa). Details on sampling by the AMS and data analysis are provided in Chen et al. (2009) and Sect. A of the Supplement. The description of other concurrent measurements and the comparisons among the measurements are provided in Sect. B of the Supplement~~ and Supplement Fig. S2~~. ~~The estimated campaign-average value of effective density (ρ_{eff}) for submicron Amazonian particles is 1390 ± 150 kg m^{-3} (Fig. S3), corresponding to the organic material density (ρ_{org}) of 1270 ± 110 kg m^{-3}.~~ Table S1 lists the regression coefficients for the multi-instrument data comparison. For a collection efficiency of unity, the AMS data agreed within measurement uncertainty with the other data sets~~. By comparison, the collection efficiency recommended for many other locations worldwide is 0.5 (Middlebrook et al., 2012).~~, which is consistent with the understanding that liquid particles do not bounce from the AMS vaporizer (Matthew et al., 2008). Images of filter samples showed that spherical organic particles, appearing as like-liquid droplets, were the main population in the submicron fraction of the ambient particle population for AMAZE-08 (Pöschl et al., 2010)~~. This observation is consistent with the collection efficiency of unity because liquid particles do not bounce from the AMS vaporizer (Matthew et al., 2008)~~.

Atomic ratios of oxygen-to-carbon (O:C), hydrogen-to-carbon (H:C), nitrogen-to-carbon (N:C), and sulfur-to-carbon (S:C), as well as the organic-mass-to-organic-carbon (OM:OC) ratios, were calculated from the high-resolution "W-mode" data (Aiken et al., 2008). The ratios

were corrected by the method of Canagaratna et al. (2015). The contributions of organonitrates and organosulfates, detected as inorganic nitrate or sulfate ions by the AMS, to the elemental ratios were negligible because their low mass concentrations (cf. Sect. A of the Supplement). ~~Corrections described by Chen et al. (2011) and Canagaratna et al. (2014) were included for organic material having keto , hydroxyl , and acid functionalities. These functionalities undergo thermally induced dehydration and decarboxylation on the AMS vaporizer, leading to increased values of $(CO^+)_{org}$:$(CO_2^+)_{org}$ and $(H_2O^+)_{org}$:$(CO_2^+)_{org}$ as compared to the values presented in Aiken et al. (2008).~~

Positive-matrix factorization (PMF; (Paatero and Tapper, 1994)) was conducted on the organic mass spectra of the medium-resolution "V-mode" data (*m*/*z* 12 to 220) taken to unit-mass resolution. The analysis used the PMF evaluation panel of Ulbrich et al. (2009) (version 4.2; "robust mode"). Further aspects of the analysis and output evaluation are provided in Sect. C of the Supplement. Because of the low mass concentrations ~~during AMAZE-08~~, the signal-to-noise ratios were insufficient for satisfactory PMF analysis of the high-resolution data. PMF results are reported herein for unit mass resolution.

The AMS mass spectra of SOM produced in the Harvard Environmental Chamber (HEC) by (i) the photooxidation of isoprene (C_5H_8), (ii) the dark ozonolysis of the monoterpene α-pinene ($C_{10}H_{16}$) (adapted from Shilling et al. (2009)), and (iii) the dark ozonolysis of the sesquiterpene β-caryophyllene ($C_{15}H_{24}$) are reported herein for the purpose of comparison to the AMAZE-08 data. Experimental details are described elsewhere (Shilling et al., 2009; King et al., 2010; Chen et al., 2011 and 2012). A library of spectra was collected at different SOM mass concentrations.

3. Results and Discussion

3.1 Mass concentrations ~~and comparisons of data sets~~

Figure 1 shows a time series of measurements by the AMS and other instruments during AMAZE-08. The AMS detects the non-refractory ~~(NR)~~ chemical components of the submicron fraction of the ambient particle population (NR-PM_1) (Fig. 1a-1c). As described in Chen et al. (2009), organic ~~Organic~~ material and sulfate were the two major components identified by the AMS, with correspondingly low concentrations of ammonium and negligible concentrations of nitrate and chloride. The campaign-average organic particle mass concentration was 0.76 ± 0.23 μg m^{-3}, corresponding to 0.45 ± 0.13 μg C m^{-3} of organic carbon and an OM:OC ratio of 1.7. ~~This concentration is lower than the range of 0.59 to 1.13 μg C m^{-3} reported for $PM_{2.5}$ in previous wet-season campaigns (Martin et al., 2010a), explained by the differences in the sampled diameter domains. Some organic material can be present in a diameter range of 1 to 2.5 μm (Pöschl et al., 2010), which was not measured in the present study.~~

The campaign-average sulfate mass concentration of 0.19 ± 0.06 μg m^{-3} agreed well with the average value of 0.~~19~~21 ± 0.06 μg m^{-3} measured by ion chromatography (IC) and the value of 0.~~21~~24 ± 0.~~04~~05 μg m^{-3} measured by particle-induced X-ray emission (PIXE) for the fine-mode (PM_2) filters. ~~The average fine-mode sulfate mass concentrations for previous campaigns ranged from 0.17 to 0.26 μg m^{-3} in the wet season, and sulfate was found predominately in the submicron range (Martin et al., 2010a). There was therefore consistency across campaigns and instruments for sulfate mass concentrations. Our data did not provide evidence for substantial contributions of organosulfate species during AMAZE-08, at least at concentrations above uncertainty levels (see further in Sect. A of the supplementary material).~~

Ammonium accounted for 2% of the submicron particle mass concentration. The

campaign-average mass concentration was 0.03 ± 0.01 μg m^{-3}, in agreement with the average value of 0.04 ± 0.01 μg m^{-3} obtained for the fine-mode filters by the IC analysis. Chloride concentrations ~~were transiently larger (up to 26 ng m^{-3}) during some periods, with~~, had a campaign-average concentration of 2 ng m^{-3}, which was consistent with the filter average, though there were transiently larger (up to 26 ng m^{-3}) during some periods. Nitrate had a campaign-average concentration of 7 ± 2 ng m^{-3}. This value was greater than the average fine-mode concentration of 4 ± 1 ng m^{-3} measured by IC, ~~possibly~~perhaps because of increased instrument uncertainties at low concentrations. Another possibility, meaning substantial evaporative losses of nitrate during filter sampling, is not anticipated for the hygroscopic, acidic particles present during the measurement periods for the prevailing relative humidity. The AMS-measured nitrate accounted for 0.6% of the total submicron particle mass concentration. ~~As a test against possible significance of organonitrates (which also fragment to the NO_x^+ ions in the AMS (Farmer et al., 2010)) to results of the present study, a limiting assumption that assigns all AMS-measured nitrate to organonitrates increases the average O:C ratio by <0.01 for the elemental analysis and corresponds to a maximum of 5% contribution of organonitrates to the total organic particle mass concentration for an assumed molecular weight of 360 g mol^{-1} (Chen et al., 2011). The low mass concentration of particle-phase organonitrates is expected because of the low prevailing NO_x concentrations and humid environment (Day et al., 2010; Liu et al., 2012).~~

Black carbon, mineral dust, and sea salt are common refractory components that are not quantified by the AMS. The multiangle absorption photometer (MAAP) instrument provides an optically based measurement of the black-carbon-equivalent (BCe) mass concentration, without size resolution (Petzold et al., 2002). The campaign-average concentration was 0.13 μg m^{-3} (Fig. 1d). Under a limiting assumption that all black carbon occurred in the submicron fraction of the

atmospheric particle population, this concentration corresponded to 11% of the submicron mass concentration (inset of Fig. 1e). The relative contribution of black carbon varied significantly during the course of AMAZE-08 (Fig. 1e), perhaps corresponding to the occasional advection of urban pollution from Manaus or biomass burning from Africa (Kuhn et al., 2010; Martin et al., 2010b; Rizzo et al., 2013). This interpretation is supported by the covariance of BCe with sulfate.

Major fine-mode (PM_2) trace elements of mineral dust, including Si, Al, Fe, and Ca, had campaign-average mass concentrations of 0.12, 0.05, 0.04, and 0.01 μg m^{-3}, respectively, as analyzed for fine-mode filter samples by PIXE. An important source of the mineral dust was long-range transport from Africa. Previous campaigns in the Amazon found that about 20% of the mineral dust occurred in the submicron domain (Fuzzi et al., 2007). Using this result for AMAZE-08 implies that mineral dust contributed about 0.1 μg m^{-3} to the average mass concentration of the submicron particle population (Malm et al., 1994). The modified pie chart is shown in Fig. S2~~S4~~. ~~The~~Moreover, the campaign-average mass concentrations of fine-mode metallic elements (V, Cr, Mn, Ni, Cu, Zn, Pb, and Mg in total of 2 ng m^{-3}) measured by PIXE were sufficiently low during AMAZE-08 to confirm the absence in the submicron particle mass concentration of significant metals from anthropogenic sources. The campaign-average mass concentration of fine-mode Na^+ measured by IC was 0.02 μg m^{-3}. This result suggests a minimal contribution of sea salt from Atlantic Ocean, at least to the submicron particle ~~mass concentration because sea salt is predominantly distributed in the supermicron domain~~population (Fuzzi et al., 2007).

Figure 1f shows the time series of the particle light scattering coefficient measured by nephelometry at 550 nm for PM_7. The elevated scattering coefficients during 22 February to 3

March 2008 were driven by elevated mineral dust concentrations in the coarse mode, along with elevated submicron sulfate, BCe, and organic material arising from the advection of the Manaus pollution plume as well as long-range transport from Africa (Sect. B of the Supplement ~~and Supplement Fig. S5)~~. Other temporal maxima corresponded to increases of submicron particle mass concentration. Figure 1g shows the elemental compositions of the submicron organic material measured by the AMS. The O:C and H:C ratios, corrected as described in Canagaratna et al. ~~(2014),~~(2015), were 0.~~59~~58 ± 0.16 (one standard deviation) and 1.~~59~~60 ± 0.18 on average, respectively. The 10/90 quantiles were 0.~~42~~40/0.~~75~~74 and 1.42/1.80, respectively. The N:C ratios were 0.03 ± 0.01~~, similar to those observed in some urban areas (Aiken et al., 2008; Docherty et al., 2011)~~.

Ammonium and sulfate mass concentrations had high correlation (R^2 = 0.95) during AMAZE-08 (Fig. ~~S6~~S3). The molar ratio of $NH_4^+ : SO_4^{2-}$ was 0.80 (Fig. 2), meaning that there was insufficient ammonium to neutralize sulfate ~~(i.e., requiring a molar ratio of 2)~~ for the submicron particle population~~.~~ and suggesting a composition close to that of ammonium bisulfate. Similar molar ratios have been reported in several previous studies in the central and northeast Amazon basin (Talbot et al., 1988, 1990; Gerab et al., 1998; Graham et al., 2003b). ~~Some of the unbalanced sulfate can be potassium sulfate (Fuzzi et al., 2007; Pöhlker et al., 2012). The fine mode mass concentration of K^+ measured by IC and PIXE was 0.03 μg m^{-3} on average. By comparison, at a deforested, pasture site in the southern parts of the Amazon basin, the particle phase ammonium can be enriched above sulfate concentrations and mainly balanced by organic acids (Trebs et al., 2005).~~

~~These earlier studies also examined the overall charge balance of the fine mode when including cations of Na^+, K^+, Ca^{2+}, and Mg^{2+} (Talbot et al., 1988, 1990; Gerab et al., 1998;~~

~~Graham et al., 2003b). For AMAZE-08, the charge concentration of inorganic anions was nearly balanced by that of the inorganic cations for the fine mode. Specifically, the species SO_4^{2-}, NO_3^-, and Cl^- contributed 93%, 5%, and 2% of the anions, respectively. The species NH_4^+, K^+, Na^+, Mg^{2+}, and Ca^{2+} contributed 40%, 20%, 15%, 15%, and 10% of the cations, respectively.~~ The AMS is unable to quantify refractory components such as K^+, Na^+, Ca^{2+}, and Mg^{2+}. Mass-diameter distributions of these ions obtained by IC analysis of samples collected by a Multi-Orifice Uniform Deposit Impactor (MOUDI) on 22 March 2008 suggest that 40% of the mass of these ions was distributed to the submicron particle fraction. For comparison, Fuzzi et al. (2007) for the wet season reported 50-60% of K^+ and Ca^{2+} in the submicron fraction, compared to the predominance of Na^+ and Mg^{2+} in the supermicron fraction. The campaign-average fine-mode mass concentrations of K^+, Ca^{2+}, Na^+, and Mg^{2+} measured by IC were 0.03, 0.01, 0.02, and 0.01 $\mu g\ m^{-3}$, respectively. The implication of the relative concentrations (i.e., sulfate concentration of $0.19 \pm 0.06\ \mu g\ m^{-3}$) is that the submicron inorganic ion composition is reasonably approximated as ammonium bisulfate during AMAZE-08.

Diel profiles of organic, sulfate, ammonium, nitrate, and chloride mass concentrations measured by the AMS are shown in Fig. 3. The temporal trends of the four species were ~~highly~~ correlated, with a minimum in mass concentrations near daybreak and a maximum in the afternoon. Nighttime rainfall efficiently removed particle mass concentration after local midnight, suggesting an absence of strong sources of submicron particles during the night. From the morning to the afternoon, photochemical production of SOM, convective mixing of particles from aloft, and regional advection sustained mass concentrations, with quick recovery after daytime rainfall. Precipitation was typically local whereas advection was typically regional at a larger scale than precipitation. The decrease and the recovery ~~as a campaign average~~of species

concentration during the afternoon resulted from frequent rain events around that time of day (e.g., Fig. ~~S7~~S4). The organic particle mass concentration increased during the day ~~increased~~ even as temperature rose and relative humidity dropped, both of which ~~can~~ provide a thermodynamic driving force for the re-partitioning of semivolatile species from the particle phase to the gas phase (Pankow, 1994). Possible explanations include (1) sufficiently strong daytime production of SOM to outweigh evaporative sinks, (2) significant production of low-volatility SOM (Ervens et al., 2011; Ehn et al., 2014), or (3) a slow evaporation rate of SOM (Vaden et al., 2011).

3.2. Mass spectra of laboratory biogenic SOM

As a reference for interpreting the AMAZE-08 measurements, Figure 4 shows the mass spectra of SOM produced in the HEC by the oxidation of isoprene, α-pinene, and β-caryophyllene for three different mass concentrations. Signals at $m/z < 60$ account for 93-97%, 80-84%, and 71-79% of the total signal intensity for the three types of SOM. The fragmentation pattern extends to higher m/z for the increasing carbon skeleton of precursor BVOC. For all three types of SOM, the relative intensities of two prominent ions, $C_2H_3O^+$ at m/z 43 and CO_2^+ at m/z 44, show opposite trends as the mass concentration increases. The former increases for elevated concentrations whereas the later decreases. Another ion at m/z 44, $C_2H_4O^+$, shows a trend similar to that of $C_2H_3O^+$. This ion accounts for 10−25%, 3−5%, and 5−10% of the signal at m/z 44 for the isoprene, α-pinene, and β-caryophyllenethe SOMs, respectively. The relative intensities of major $C_xH_y^+$ ions, such as CH_3^+ at m/z 15, $C_2H_3^+$ at m/z 27, $C_3H_3^+$ at m/z 39, and $C_3H_5^+$ at m/z 41, typically increase as concentration increases. The most intense $C_xH_y^+$ ions at $m/z >$ 80 for the three types of biogenic SOM is $C_7H_7^+$ at m/z 91, which does not occur in the spectra for fresh emissions such as diesel exhaust, cooking, and biomass burning but is similar to the spectra

for aged primary emissions (Chirico et al., 2010; He et al., 2010; Ortega et al., 2013).

Compared to the spectra of the other types of biogenic SOM, isoprene-derived SOM under HO_2-dominant conditions has a unique signature. "HO_2-dominant" refers to the fate of peroxy radicals with respect to reaction with HO_2 or NO. The relative intensities of CHO^+ at *m/z* 29, CH_2O^+ at *m/z* 30, CH_3O^+ at *m/z* 31, $C_3H_6O_2^+$ at *m/z* 74, and $C_3H_7O_2^+$ at *m/z* 75 in the spectra of isoprene-derived SOM are much greater, and the contributions of $C_xH_y^+$ ions are less, especially for $m/z > 65$. Moreover, *m/z* 82 that mainly consists of $C_3H_5O^+$ appears to be the most intense peak for $m/z \geq 75$. This fragment has been suggested as a characteristic fragment of isoprene-derived SOM (Robinson et al., 2011). Isoprene-derived SOM also does not follow the empirical linear relationship between O:C and I_{44}:I_{org} described by Aiken et al. (2008) (Fig. S5), indicating that deriving O:C from I_{44}:I_{org} requires careful judgments on the contribution of isoprene-derived SOM.

~~3.2~~3.3 Multivariate factor analysis of the organic mass spectra

Multivariate analysis by ~~positive matrix factorization (~~PMF~~)~~ of the temporal series of the organic component of the mass spectra was carried out for $12 \leq m/z \leq 220$ at unit-mass resolution. In overview, four statistical factors were identified and labeled as HOA, OOA-1, OOA-2, and OOA-3 (Fig. ~~4~~5) ~~(cf. Sect. C of the supplementary material)~~. ~~The~~ These four factors ~~HOA, OOA-1, OOA-2, and OOA-3~~ respectively accounted for 2%, 18%, 14%, and 66% of the variance in the data matrix, ~~implying~~with a residual variance of <1%. ~~Time~~The time series of the ~~mass concentration~~loading of each statistical factor are shown in Fig. ~~5~~6. ~~The four factors HOA, OOA-1, OOA-2, and OOA-3 represented on average 14%, 14%, 34%, and 38% of the organic particle mass concentration.~~ By definition, the mass spectrum of the organic chemical component itself was at any time point a linear mix of the statistical factors, plus residual.

The HOA factor (Fig. ~~4a~~5a) was dominated by the ion series $C_nH^+_{2n+1}$, $C_nH^+_{2n-1}$, and $C_nH^+_{2n-3}$ (*m*/*z* 27, 29, 39, 41, 43, 55, 57, 67, 69…), similar to that reported for other locations (e.g., Zhang et al., 2005; Docherty et al., 2011; Robinson et al., 2011) and to that observed for engine exhaust (Canagaratna et al., 2004~~)~~; Chirico et al., 2010). This statistical factor is typically taken as an organic component associated with fossil fuel combustion emissions that have not undergone substantial atmospheric oxidation. This factor was especially prevalent in the early part of the experiment. During this time period, other pollution tracers such as sulfate and NO_x were also at elevated concentrations. Regional pollution from Manaus and local emissions (e.g., nearby roads, highway, generator, and pump oil) were plausible contributors to the ~~mass concentration~~loading of the HOA factor (Ahlm et al., 2009; Rizzo et al., 2013)~~, which accounted for 14% of the organic mass concentration as a campaign average. For comparison, other studies have reported that the HOA factor accounted for 0 to 21% of the mass concentrations for remote locations and up to 53% for urban regions (Jimenez et al., 2009)~~.

The factors OOA-1, OOA-2, and OOA-3 were ranked by the f_{44}:f_{43} ratios (high to low) and labeled based on Zhang et al. (2011), where $f_{m/z}$ represents the fractional contribution of the signal intensity at *m*/*z* to the statistical factor. The signal intensity was dominated at *m*/*z* 44 by the CO_2^+ fragment and at *m*/*z* 43 by the $C_2H_3O^+$ and $C_3H_7^+$ fragments. The f_{44}:f_{43} ratio has been used in some settings as a surrogate for the extent of oxidation (i.e., so-called ‘atmospheric aging’) of SOM (Ng et al., 2010 and 2011).

The OOA-1 factor had the feature of a singularly dominant peak at *m*/*z* 44 (Fig. ~~4b~~5b) ~~and was believed to be mainly associated with long-range transport of African biomass burning~~. ~~A dominant peak at *m*/*z* 44~~This marker has been linked to organic material that has undergone extensive oxidation during a prolonged atmospheric residence time (on order of 10 days) ~~(Ng et~~

~~al., 2010)~~(Ng et al., 2010; Lambe et al., 2011). This factor is consistent with an association to finding of highly-oxidized~~As described in Chen et al. (2009),~~ organic material ~~was~~ delivered by long-range transport, as occurred during some periods of AMAZE-08~~, and this material was continuously oxidized during the advection process~~(Chen et al., 2009). The source of this material was plausibly ~~Africa~~African biomass burning, as supported by concurrent lidar measurements (Baars et al., 2011) and satellite observations (Ben-Ami et al., 2010). ~~South American biomass~~Biomass burning in South America was much less significant during the wet season (Martin et al., 2010b). The ~~mass concentration~~correlations of the statistical loadings of the OOA-1 factor ~~correlated~~ with the measured mass concentrations of biomass burning tracers, such as chloride (R^2 = 0.52), potassium (R^2 = 0.35), and black carbon (R^2 = 0.43) in the submicron particle population, were not high, possibly because of the mixing of sources to these tracers such as primary biological particles (i.e., contributing chloride and potassium) and regional pollution from Manaus to (i.e., black carbon)~~ (Fig. 5b) (Cubison et al., 2011)~~. These correlation value were, however, significantly greater than those of the other three factors (HOA, OOA2, and OOA-3) with the tracers (i.e., $R^2 < 0.10$ for chloride, $R^2 < 0.02$ for potassium, and $R^2 < 0.20$ for black carbon) (Fig. 6b). Elevated sulfate mass concentrations were also observed during periods having high OOA-1 loadings (Fig. 1b).~~For comparison, the mass concentrations of the other three factors (HOA, OOA2, and OOA-3) did not correlate with these tracers (R^2 < 0.10 for chloride; R^2 < 0.02 for potassium; and R^2 < 0.20 for black carbon with each of the three factors). The sulfate mass concentration was also elevated when the OOA-1 concentration was high (Fig. 1). The relative intensity of *m/z* 60, which is the typical marker for fresh biomass burning and attributed to the product levoglucosan, was less than the recommended threshold value of 0.35% for background conditions (Docherty et al., 2008) (Fig. S8). As biomass burning particles~~

become more oxidized due to ongoing atmospheric reactions downwind of African fires, the peak at *m/z* 60 was observed to diminish and that at *m/z* 44 was observed to increase (Capes et al., 2008).

Features of the OOA-2 factor included (1) a f_{44}:f_{43} ratio greater than unity and (2) a prominentcharacteristic peak at *m/z* 82 distinct from adjacent ions along with elevated mainly consisting of $C_3H_5O^+$. This peak was the most abundant for *m/z* 53≥ 75 (Fig. 4c5c). These features wereIt is similar to thosethat reported for PMF factors identified in the tropical rainforest of Borneo (OP3named as the "82Fac" factor) (Robinson et al., 2011), the rural area of southwest Ontario, Canada (BAQS-Met 2007named as the "UNKN" factor) (Slowik et al., 2011), and the isoprene-rich downtown Atlanta (isoprene-rich), Georgia, USA (SEARCHnamed as the "IEPOX-OA" factor) (Budisulistiorini et al., 2013). The OOA-2 factor of AMAZE-08 accounted for on average 34% of the organic mass concentration, compared to 23% for Borneo (named as the "83Fac" factor), up to 50% for Ontario during periods of high isoprene emissions (named as the "UNKN" factor), and 33% for Atlanta (named as the "IEPOX-OA" factor). Robinson et al. (2011) concluded that this factor derived from SOM produced by isoprene photo-oxidation. In agreement, the time series of OOA-2 loading correlated with isoprene concentration (R^2 = 0.65) as well as with the sum concentration of first-generation isoprene oxidation products, specifically MVK + MACR (R^2 = 0.74) (Fig. 6c). The characteristic *m/z* 82 also occurred in the spectra of our isoprene SOM produced in the presence of neutral sulfate particles at 40% RH (Fig. 4a). Laboratory studies demonstrated that the reactive-uptake of photo-oxidation products of isoprene, particularly IEPOX, in the presence of acidic particles contribute to the *m/z* 82 signal detected by the AMS (Lin et al., 2012; Budisulistiorini et al., 2013; Liu et al., 2014). Even so, the spectra of isoprene SOM or IEPOX SOM produced in the laboratory have some important

differences with the statistical factories (i.e., "OOA-2" of this study and "82Fac", "UNKN", and "IEPOX-OA" of earlier studies) derived from atmospheric data sets. In particular, there are significant differences at *m*/*z* 29 and *m*/*z* 39 through *m*/*z* 44. The values of f_{44} of the laboratory results are approximately 25% of those of the cited PMF factors. One possible explanation for these differences is that the laboratory experiments did not capture the full range of atmospheric processes, such as possible synergistic chemistry among the range of atmospheric precursors, aqueous-phase processing, and photochemistry under a range of HO_2:NO ratios (Ervens et al., 2011; Emanuelsson et al., 2013; Liu et al., 2013; Nguyen et al., 2014). In particular, the laboratory experiments were typically carried out at low relative humidity. The atmosphere during AMAZE-08 was humid (89 to 100% RH; 25 to 75% quantiles). Pöhlker et al. (2012) showed evidence of multiphase processing in the larger accumulation mode particles. The oxidized material produced by aqueous-phase oxidation (e.g., dicarboxylic acids (Lim et al., 2010)) may explain the higher f_{44} in the OOA-2 factor compared to the laboratory spectra. In summary, the OOA-2 factor during AMAZE-08 was interpreted as SOM produced by the reactive uptake of isoprene photo-oxidation products, including possible aqueous-phase oxidation in haze, fog, and cloud droplets.

~~Lin et al. (2012) demonstrated the formation of 3-methyltetrahydrofuran-3,4-diols as a contributor to the *m*/*z* 82 signal detected by the AMS and dervied from the acid-catalyzed intramolecular rearrangement of IEPOX isomers in the particle phase. Although IEPOX was not directly measured during AMAZE-08, the time series of the OOA-2 mass concentration correlated with isoprene concentration (R^2 = 0.65) as well as with the sum concentration of first-generation isoprene oxidation products, specifically MVK + MACR (R^2 = 0.74) (Fig. 5c). Budisulistiorini et al. (2013) showed that the OOA-2 factor resembled the spectrum of the~~

~~organic material produced in chamber experiments by the reactive uptake of gaseous IEPOX isomers by acidic particles, especially with respect to *m/z* 82. Kuwata et al. (2014) confirmed this result in another chamber study. Uptake of isoprene IEPOX isomers depends on the liquid water content and the inorganic composition of the particles (Lin et al., 2012; Budisulistiorini et al., 2013; Nguyen et al., 2014). The atmosphere during AMAZE-08 was humid, HO_2-dominant, and isoprene-rich, with the presence of acidic submicron particles. These conditions favored the gas-phase production and the particle-phase reactive uptake of IEPOX isomers (Surratt et al., 2010), which were associated with *m/z* 82 by AMS characterization.~~

~~Particle-phase production pathways for secondary organic material in haze, fog, and cloud droplets can be several-fold. In addition to IEPOX uptake and reaction, aqueous-phase chemistry of water-soluble products of gas-phase photochemistry can produce lower-volatility oxidized organic material, such as oxalate and dicarboxylic acids (Ervens et al., 2011). Pöhlker et al. (2012) reported an abundance of carboxylate functionalities of Amazonian particles consistent with aqueous processing. The oxidized material produced by aqueous-phase oxidation can help to explain the higher f_{44} in the OOA-2 factor compared to the mass spectra observed in laboratory experiments that studied the uptake of IEPOX isomers (Lin et al., 2012; Budisulistiorini et al., 2013; Nguyen et al., 2014). Pöhlker et al. (2012) also showed evidence of multiphase processing, i.e., a COOH-rich core and a C-OH-rich shell for single particles. The C-OH-rich shell was consistent with the production of polyols by IEPOX uptake and reaction (Lin et al., 2012). The OOA-2 factor during AMAZE-08 therefore plausibly represented the reactive uptake of IEPOX isomers and other gas-phase species by haze, fog, and cloud droplets.~~

The OOA-3 factor had ~~distinct peaks~~a prominent peak at *m/z* 43~~, 55, and~~ (Fig. 5d). For *m/z* > 80, the most intense peak occurred at *m/z* 91~~ (Fig. 4d). These features were also prominent~~

~~in reference~~. The OOA-3 factor had similarities to the mass spectra recorded for biogenic SOM produced ~~by oxidation of BVOCs in an environmental chamber for~~under conditions relevant to the Amazon basin ~~(Fig. 6) (see further in Sect. D of the Supplement) (Shilling et al., 2009; Chen et al., 2011 , 2012). In these laboratory studies, dry ammonium sulfate seed particles were used. SOM derived from isoprene (C_5) .~~ Specifically, SOM produced from isoprene under laboratory conditions had a prominent peak at *m*/*z* 43~~.~~ (Fig. 4a). Mass spectra of SOM derived from precursors of monoterpene α-pinene ~~(C_{10})~~ and sesquiterpene β-caryophyllene ~~(C_{15})~~ had ~~prominent peaks~~similar patterns as OOA-3 at *m*/*z* 55 and *m*/*z* 91. A linear combination of the three chamber spectra largely reproduced the OOA-3 factor (Fig. 7; 50% isoprene-derived SOM, 30% α-pinene-derived SOM, and 20% β-caryophylene-derived SOM). The intensity at *m*/*z* 29, however, was overestimated by the linear combination. The remarkable result is that the ambient factor could to large extent be explained by just three laboratory data sets given the wide range of BVOC precursor compounds that can contribute to SOM production in the Amazon basin. The explanation is three-fold, one that isoprene is the dominant BVOC for this rain forest, two that the AMS breaks complex molecules into simpler building blocks by electron-impact ionization, and three that the higher-order C_{10}, C_{15}, and possibly C_{20} BVOCs are all assembled biochemically from the isoprene (C_5) monomer. Moreover, the temporal variation of the OOA-3 loading tracked that of the BVOC concentrations (Fig. 6d).~~S9; 50% isoprene SOM, 30% α-pinene SOM, and 20% β-caryophylene SOM). Other studies have also reported similar features for SOM derived from β-pinene and limonene as well as various tree emissions under chamber conditions (Kiendler-Scharr et al., 2009; Kostenidou et al., 2009). A plausible interpretation therefore is that the~~ The OOA-3 statistical factor was therefore interpreted as associated with freshly produced SOM similar to that produced in the chamber experiments, ~~i.e.,~~meaning on a

timescale of several hours by a mechanism of gas-to-particle partitioning of the BVOC oxidation products. ~~In support of this interpretation, the temporal variation of the OOA-3 mass concentration tracked that of the BVOC concentrations (Fig. 5d). The OOA-3 factor contributed on average to about 38% of the organic particle mass concentration.~~

Figure ~~7~~8 shows the campaign-average diel profiles of the factor loadings~~mass concentrations of the PMF factors~~. The HOA ~~mass concentration showed~~loading had a daytime minimum, suggesting the buildup of local pollution during the night and the removal by convective mixing during the day. ~~The OOA-1 mass concentration~~In support of this interpretation, the nocturnal boundary layer was approximately 100 m or less. At daybreak, the boundary layer rapidly developed, reaching on order of 1000 m by local noon around the site (Martin et al., 2010b). The OOA-1 loading peaked around noon without great variation throughout the day. This temporal behavior is expected for homogeneous mixing in the atmospheric column without in situ sources, ~~i.e.,~~such as for material arriving by long-range transport. The small daytime increase was consistent with the daytime convective downward mixing of older, oxidized particles from aloft. By comparison, the OOA-2 and OOA-3 ~~mass concentrations~~loadings peaked in the early afternoon while the BVOC concentrations were high (cf. Fig. 3c of Chen et al. (2009)). This temporal behavior was consistent with the photochemically driven production of SOM.

Figure ~~8~~9 shows the time series of fractional contribution by each of the four statistical factors identified by PMF analysis. ~~The relative importance of processes as contributors to the organic particle mass concentration differed with time. As an example, Figure 8 highlights two focus periods.~~On average the relative loadings of HOA, OOA-1, OOA-2, and OOA-3 were 14%, 14%, 34%, and 38%, respectively. For comparison, other studies reported 0 to 21% of HOA for

remote locations (Jimenez et al., 2009) and 23% to 50% of OOA-2 (named as "82Fac", "UNKN", and "IEPOX-OA" in earlier studies) (Robinson et al., 2011; Slowik et al., 2011; Budisulistiorini et al., 2013). Figure 9 shows that the relative importance of each process as a contributor differed with time and highlights two focus periods. Precipitation and temperature were the major meteorological factors that differed between the two periods. The first period was sunny, warmer with occasional clouds, and the second period had frequent heavy rainfall events. Long-range back-trajectory analyses presented in Martin et al. (2010b) showed that the air masses consistently arrived from the equatorial Atlantic Ocean passing as northeasterlies through the Amazon basin. Local measurements showed that the daytime winds mainly came from the north and northeast (Fig. 9, top). During the first period, the average fractional contribution by the OOA-2 factor was five times greater than that of the OOA-3 factor. During the second period, by comparison, the fractional contribution by the OOA-3 factor was three times greater than that of the OOA-2 factor. The average organic mass concentrations of the two periods were 1.84 and 0.59 μg m^{-3}, respectively. ~~As a campaign average, the mass fractions contributed by the OOA-2 and OOA-3 factors were approximately 1:1. The mass concentrations were in a ratio of 1.4:1.~~

Figure 9 shows that the loading fraction of the OOA-2 factor consistently dropped following heavy rainfall events, suggesting more efficient in-cloud or below-cloud scavenging for the types of material represented by OOA-2 than for those types represented by OOA-3. This finding further supports the interpretation that the OOA-2 factor represents, at least in part, aqueous-phase production pathways because SOM produced in this way has greater water solubility and hence greater wet deposition rates than SOM produced freshly by gas-to-particle condensation, as interpreted for the OOA-3 factor. Figure 9 also shows that the mode diameter of

organic material in period 1, which has a higher OOA-2 loading fraction, is significantly larger than that in period 2, which has a higher OOA-3 loading fraction. Aqueous-phase processing is anticipated to add additional organic material that results in larger mode diameters after dehydration.

4. Conclusions

~~The submicron~~Submicron particle mass concentration in the Amazonian rainforest during the wet season of 2008 was dominated by organic material. The environment was humid, HO_2-dominant, isoprene-rich, with the presence of acidic particles in the submicron fraction of the atmospheric ~~aerosol. The time series of the mass spectra of the organic component of the submicron particles was analyzed by positive matrix factorization. Four statistical factors labeled HOA, OOA-1, OOA-2,~~particle population. Factors OOA-2 and OOA-3 were identified~~. The HOA factor was interpreted as representing regional and local pollution and accounted for 14% of the organic particle mass concentration. The OOA-1 factor, accounting for another 14% of the organic particle mass concentration, was highly oxidized and plausibly related to long-range transport of African biomass burning particles. The OOA-2 and OOA-3~~ in the patterns of the collected mass spectra. These factors were ~~both~~ interpreted as tied to the in-basin production of biogenic ~~SOM~~ secondary organic material and together accounted for >70% of the ~~organic particle mass concentration (Fig. 8).~~factor loadings, with the balance from HOA and OOA-1. The OOA-2 factor was ~~consistent~~implicated as associated with the reactive uptake of isoprene oxidation products ~~such as IEPOX by~~ , especially of epoxydiols to acidic ~~aerosol particles, including~~ haze, fog~~, and~~ or cloud droplets. The OOA-3 factor ~~had mass spectral features of freshly formed biogenic SOM, believed~~was consistent with an association to ~~represent gas-to-particle condensation followed by~~ the fresh production of SOM by a mechanism of gas-phase

oxidation of ~~gas-phase~~ BVOCs~~. According to this interpretation, the OOA-2 factor was associated with sustained particle-phase SOM production, and the OOA-3 factor was associated with sporadic, episodic SOM production by processes of~~ followed by gas-to-particle conversion~~.~~ ~~Processes are depicted in Fig. 9 concerning the production and further reactions of SOM.~~ of the oxidation products. Although multivariate statistical factors do not correspond to segregated individual chemical components (e.g., unlike molecules or families of molecules), the factors nevertheless can be indicative of the relative importance of different atmospheric emissions and process pathways. With this caveat in mind, the PMF analysis herein finds that the factor ~~mass concentrations~~loadings were, on average, in a ratio of 1.4:1 for ~~the~~ OOA-2 compared to ~~the~~ OOA-3 ~~pathway~~ and were alternately dominated ~~alternatively~~in different periods of AMAZE-08 by the OOA-2 and OOA-3 ~~components, suggesting~~. These findings suggest a comparable importance of gas-phase and particle-phase (including haze, fog, and cloud droplets) production of SOM during the study period.

Acknowledgments. Support was received from the USA National Science Foundation, the German Max Planck Society, and Brazilian CNPq and FAPESP agencies. QC acknowledges a NASA Earth and Space Science Fellowship. DKF acknowledges a NOAA Global Change Fellowship. TP acknowledges the CNPq grant 552831/2006-9. PA acknowledges FAPESP projects 2008/58100-2, 2010/52658-1, 2011/50170-4, 2012/14437-9. We thank the INPA LBA central office in Manaus for logistical support during AMAZE-08. We thank John Jayne ~~and~~, Joel Kimmel ~~from Aerodyne Research, Inc.,~~ Johannes Schneider, and Soeren Zorn for helping with ~~the~~ sampling and aspects of data ~~quality control~~analysis.

References

Ahlm, L., Nilsson, E. D., Krejci, R., Martensson, E. M., Vogt, M., and Artaxo, P.: Aerosol number fluxes over the Amazon rain forest during the wet season, Atmos. Chem. Phys., 9, 9381-9400, 2009.

Aiken, A. C., Decarlo, P. F., Kroll, J. H., Worsnop, D. R., Huffman, J. A., Docherty, K. S., Ulbrich, I. M., Mohr, C., Kimmel, J. R., Sueper, D., Sun, Y., Zhang, Q., Trimborn, A., Northway, M., Ziemann, P. J., Canagaratna, M. R., Onasch, T. B., Alfarra, M. R., Prevot, A. S. H., Dommen, J., Duplissy, J., Metzger, A., Baltensperger, U., and Jimenez, J. L.: O/C and OM/OC ratios of primary, secondary, and ambient organic aerosols with high-resolution time-of-flight aerosol mass spectrometry, Environ. Sci. Technol., 42, 4478-4485, 10.1021/es703009q, 2008.

Andreae, M. O., Berresheim, H., Bingemer, H., Jacob, D. J., Lewis, B. L., Li, S. M., and Talbot, R. W.: The atmospheric sulfur cycle over the Amazon Basin. 2. Wet season, J. Geophys. Res., 95, 16813-16824, 1990.

Andreae, M. O.: Aerosols before pollution, Science, 315, 50-51, 10.1126/science.1136529, 2007.

Baars, H., Ansmann, A., Althausen, D., Engelmann, R., Artaxo, P., Pauliquevis, T., and Souza, R.: Further evidence for significant smoke transport from Africa to Amazonia, Geophys. Res. Lett., 38, L20802, 10.1029/2011GL049200, 2011.

Ben-Ami, Y., Koren, I., Rudich, Y., Artaxo, P., Martin, S. T., and Andreae, M. O.: Transport of North African dust from the Bodele depression to the Amazon Basin: a case study, Atmos. Chem. Phys., 10, 7533-7544, 10.5194/acp-10-7533-2010, 2010.

Budisulistiorini, S. H., Canagaratna, M. R., Croteau, P. L., Marth, W. J., Baumann, K., Edgerton, E. S., Shaw, S. L., Knipping, E. M., Worsnop, D. R., Jayne, J. T., Gold, A., and Surratt, J. D.: Real-time continuous characterization of secondary organic aerosol derived from isoprene epoxydiols in downtown Atlanta, Georgia, using the Aerodyne aerosol chemical speciation monitor, Environ. Sci. Technol., 47, 5686-5694, 10.1021/es400023n, 2013.

Canagaratna, M. R., Jayne, J. T., Ghertner, D. A., Herndon, S., Shi, Q., Jimenez, J. L., Silva, P. J., Williams, P., Lanni, T., Drewnick, F., Demerjian, K. L., Kolb, C. E., and Worsnop, D. R.: Chase studies of particulate emissions from in-use New York City vehicles, Aerosol Sci. Technol., 38, 555-573, Doi 10.1080/02786820490465504, 2004.

Canagaratna, M. R., Jimenez, J. L., ~~Chen, Q., Massoli, P., Kessler, S., Hildebrandt, L., et al.: Improved calibration of O/C and H/C ratios obtained by Aerosol Mass Spectrometry of organic species, In preparation, 2014~~Kroll, J. H., Chen, Q., Kessler, S. H., Massoli, P., Hildebrandt Ruiz, L., Fortner, E., Williams, L. R., Wilson, K. R., Surratt, J. D., Donahue, N. M., Jayne, J. T., and Worsnop, D. R.: Elemental ratio measurements of organic compounds using aerosol mass spectrometry: characterization, improved calibration, and implications, Atmos. Chem. Phys., 15, 253-272, 10.5194/acp-15-253-2015, 2015.

~~Capes, G., Johnson, B., McFiggans, G., Williams, P. I., Haywood, J., and Coe, H.: Aging of biomass burning aerosols over West Africa: Aircraft measurements of chemical composition,~~

microphysical properties, and emission ratios, J. Geophys. Res., 113, D00C15, 10.1029/2008jd009845, 2008.

Chen, Q., Farmer, D. K., Schneider, J., Zorn, S. R., Heald, C. L., Karl, T. G., Guenther, A., Allan, J. D., Robinson, N., Coe, H., Kimmel, J. R., Pauliquevis, T., Borrmann, S., Poschl, U., Andreae, M. O., Artaxo, P., Jimenez, J. L., and Martin, S. T.: Mass spectral characterization of submicron biogenic organic particles in the Amazon Basin, Geophys. Res. Lett., 36, L20806, 10.1029/2009gl039880, 2009.

Chen, Q., Liu, Y., Donahue, N. M., Shilling, J. E., and Martin, S. T.: Particle-phase chemistry of secondary organic material: Modeled compared to measured O:C and H:C elemental ratios provide constraints, Environ. Sci. Technol., 45, 4763-4770, 10.1021/es104398s, 2011.

Chen, Q., Li, Y. L., McKinney, K. A., Kuwata, M., and Martin, S. T.: Particle mass yield from β-caryophyllene ozonolysis, Atmos. Chem. Phys., 12, 3165-3179, 10.5194/acp-12-3165-2012, 2012.

Chirico, R., DeCarlo, P. F., Heringa, M. F., Tritscher, T., Richter, R., Prevot, A. S. H., Dommen, J., Weingartner, E., Wehrle, G., Gysel, M., Laborde, M., and Baltensperger, U.: Impact of aftertreatment devices on primary emissions and secondary organic aerosol formation potential from in-use diesel vehicles: results from smog chamber experiments, Atmos. Chem. Phys., 10, 11545-11563, 10.5194/acp-10-11545-2010, 2010.

Claeys, M., Graham, B., Vas, G., Wang, W., Vermeylen, R., Pashynska, V., et al.: Formation of secondary organic aerosols through photooxidation of isoprene, Science, 303, 1173-1176, 10.1126/science.1092805, 2004.

Claeys, M., Kourtchev, I., Pashynska, V., Vas, G., Vermeylen, R., Wang, W., et al.: Polar organic marker compounds in atmospheric aerosols during the LBA-SMOCC 2002 biomass burning experiment in Rondonia, Brazil: sources and source processes, time series, diel variations and size distributions, Atmos. Chem. Phys., 10, 9319-9331, 10.5194/acp-10-9319-2010, 2010.

Cubison, M. J., Ortega, A. M., Hayes, P. L., Farmer, D. K., Day, D., Lechner, M. J., et al.: Effects of aging on organic aerosol from open biomass burning smoke in aircraft and laboratory studies, Atmos. Chem. Phys., 11, 12049-12064, 10.5194/acp-11-12049-2011, 2011.

Day, D. A., Liu, S., Russell, L. M., and Ziemann, P. J.: Organonitrate group concentrations in submicron particles with high nitrate and organic fractions in coastal southern California, Atmos. Environ., 44, 1970-1979, 10.1016/j.atmosenv.2010.02.045, 2010.

Docherty, K. S., Stone, E. A., Ulbrich, I. M., DeCarlo, P. F., Snyder, D. C., Schauer, J. J., et al.: Apportionment of primary and secondary organic aerosols in southern California during the 2005 Study of Organic Aerosols in Riverside (SOAR-1), Environ. Sci. Technol., 42, 7655-7662, 10.1021/es8008166, 2008.

Docherty, K. S., Aiken, A. C., Huffman, J. A., Ulbrich, I. M., DeCarlo, P. F., Sueper, D., Worsnop, D. R., Snyder, D. C., Peltier, R. E., Weber, R. J., Grover, B. D., Eatough, D. J.,

Williams, B. J., Goldstein, A. H., Ziemann, P. J., and Jimenez, J. L.: The 2005 Study of Organic Aerosols at Riverside (SOAR-1): instrumental intercomparisons and fine particle composition, Atmos. Chem. Phys., 11, 12387-12420, 10.5194/acp-11-12387-2011, 2011.

Ehn, M., Thornton, J. A., Kleist, E., Sipila, M., Junninen, H., Pullinen, I., Springer, M., Rubach, F., Tillmann, R., Lee, B., Lopez-Hilfiker, F., Andres, S., Acir, I. H., Rissanen, M., Jokinen, T., Schobesberger, S., Kangasluoma, J., Kontkanen, J., Nieminen, T., Kurten, T., Nielsen, L. B., Jorgensen, S., Kjaergaard, H. G., Canagaratna, M., Dal Maso, M., Berndt, T., Petaja, T., Wahner, A., Kerminen, V. M., Kulmala, M., Worsnop, D. R., Wildt, J., and Mentel, T. F.: A large source of low-volatility secondary organic aerosol, Nature, 506, 476-479, 10.1038/nature13032, 2014.

Elbert, W., Taylor, P. E., Andreae, M. O., and Poschl, U.: Contribution of fungi to primary biogenic aerosols in the atmosphere: wet and dry discharged spores, carbohydrates, and inorganic ions, Atmos. Chem. Phys., 7, 4569-4588, 10.5194/acp-7-4569-2007, 2007.

Emanuelsson, E. U., Hallquist, M., Kristensen, K., Glasius, M., Bohn, B., Fuchs, H., Kammer, B., Kiendler-Scharr, A., Nehr, S., Rubach, F., Tillmann, R., Wahner, A., Wu, H. C., and Mentel, T. F.: Formation of anthropogenic secondary organic aerosol (SOA) and its influence on biogenic SOA properties, Atmos. Chem. Phys., 13, 2837-2855, 10.5194/acp-13-2837-2013, 2013.

Ervens, B., Turpin, B. J., and Weber, R. J.: Secondary organic aerosol formation in cloud droplets and aqueous particles (aqSOA): a review of laboratory, field and model studies, Atmos. Chem. Phys., 11, 11069-11102, 10.5194/acp-11-11069-2011, 2011.

~~Farmer, D. K., Matsunaga, A., Docherty, K. S., Surratt, J. D., Seinfeld, J. H., Ziemann, P. J., and Jimenez, J. L.: Response of an aerosol mass spectrometer to organonitrates and organosulfates and implications for atmospheric chemistry, Proc. Natl. Acad. Sci. U. S. A., 107, 6670-6675, 10.1073/pnas.0912340107, 2010.~~

Fuzzi, S., Decesari, S., Facchini, M. C., Cavalli, F., Emblico, L., Mircea, M., Andreae, M. O., Trebs, I., Hoffer, A., Guyon, P., Artaxo, P., Rizzo, L. V., Lara, L. L., Pauliquevis, T., Maenhaut, W., Raes, N., Chi, X. G., Mayol-Bracero, O. L., Soto-Garcia, L. L., Claeys, M., Kourtchev, I., Rissler, J., Swietlicki, E., Tagliavini, E., Schkolnik, G., Falkovich, A. H., Rudich, Y., Fisch, G., and Gatti, L. V.: Overview of the inorganic and organic composition of size-segregated aerosol in Rondonia, Brazil, from the biomass-burning period to the onset of the wet season, J. Geophys. Res., 112, D01201, 10.1029/2005JD006741, 2007.

Gerab, F., Artaxo, P., Gillett, R., and Ayers, G.: PIXE, PIGE and ion chromatography of aerosol particles from northeast Amazon Basin, Nucl Instrum Meth B, 136, 955-960, 1998.

Graham, B., Guyon, P., Taylor, P. E., Artaxo, P., Maenhaut, W., Glovsky, M. M., Flagan, R. C., and Andreae, M. O.: Organic compounds present in the natural Amazonian aerosol: Characterization by gas chromatography-mass spectrometry, J. Geophys. Res., 108, 4766, 10.1029/2003jd003990, 2003a.

Graham, B., Guyon, P., Maenhaut, W., Taylor, P. E., Ebert, M., Matthias-Maser, S., Mayol-Bracero, O. L., Godoi, R. H. M., Artaxo, P., Meixner, F. X., Moura, M. A. L., Rocha, C., Van

Grieken, R., Glovsky, M. M., Flagan, R. C., and Andreae, M. O.: Composition and diurnal variability of the natural Amazonian aerosol, J. Geophys. Res., 108, 4765, 10.1029/2003JD004049, 2003b.

Gunthe, S. S., King, S. M., Rose, D., Chen, Q., Roldin, P., Farmer, D. K., Jimenez, J. L., Artaxo, P., Andreae, M. O., Martin, S. T., and Pöschl, U.: Cloud condensation nuclei in pristine tropical rainforest air of Amazonia: size-resolved measurements and modeling of atmospheric aerosol composition and CCN activity, Atmos. Chem. Phys., 9, 7551-7575, 10.5194/acp-9-7551-2009, 2009.

He, L. Y., Lin, Y., Huang, X. F., Guo, S., Xue, L., Su, Q., Hu, M., Luan, S. J., and Zhang, Y. H.: Characterization of high-resolution aerosol mass spectra of primary organic aerosol emissions from Chinese cooking and biomass burning, Atmos. Chem. Phys., 10, 11535-11543, DOI 10.5194/acp-10-11535-2010, 2010.

IPCC: *Climate Change 2013: The Physical Science Basis. Contribution of Working Group I to the Fifth Assessment Report of the Intergovernmental Panel on Climate Change* [Stocker, T.F., D. Qin, G.-K. Plattner, M. Tignor, S.K. Allen, J. Boschung, A. Nauels, Y. Xia, V. Bex and P.M. Midgley (eds.)], Cambridge University Press, Cambridge, United Kingdom and New York, NY, USA, 1535 pp, 2013.

Jimenez, J. L., Canagaratna, M. R., Donahue, N. M., Prevot, A. S. H., Zhang, Q., Kroll, J. H., DeCarlo, P. F., Allan, J. D., Coe, H., Ng, N. L., Aiken, A. C., Docherty, K. S., Ulbrich, I. M., Grieshop, A. P., Robinson, A. L., Duplissy, J., Smith, J. D., Wilson, K. R., Lanz, V. A., Hueglin, C., Sun, Y. L., Tian, J., Laaksonen, A., Raatikainen, T., Rautiainen, J., Vaattovaara, P., Ehn, M., Kulmala, M., Tomlinson, J. M., Collins, D. R., Cubison, M. J., Dunlea, E. J., Huffman, J. A., Onasch, T. B., Alfarra, M. R., Williams, P. I., Bower, K., Kondo, Y., Schneider, J., Drewnick, F., Borrmann, S., Weimer, S., Demerjian, K., Salcedo, D., Cottrell, L., Griffin, R., Takami, A., Miyoshi, T., Hatakeyama, S., Shimono, A., Sun, J. Y., Zhang, Y. M., Dzepina, K., Kimmel, J. R., Sueper, D., Jayne, J. T., Herndon, S. C., Trimborn, A. M., Williams, L. R., Wood, E. C., Middlebrook, A. M., Kolb, C. E., Baltensperger, U., and Worsnop, D. R.: Evolution of organic aerosols in the atmosphere, Science, 326, 1525-1529, 10.1126/science.1180353, 2009.

Karl, T., Guenther, A., Turnipseed, A., Tyndall, G., Artaxo, P., and Martin, S.: Rapid formation of isoprene photo-oxidation products observed in Amazonia, Atmos. Chem. Phys., 9, 7753-7767, 2009.

~~Kiendler-Scharr, A., Zhang, Q., Hohaus, T., Kleist, E., Mensah, A., Mentel, T. F., et al.: Aerosol mass spectrometric features of biogenic SOA: Observations from a plant chamber and in rural atmospheric environments, Environ. Sci. Technol., 43, 8166-8172, 10.1021/es901420b, 2009.~~

~~Kostenidou, E., Lee, B. H., Engelhart, G. J., Pierce, J. R., and Pandis, S. N.: Mass spectra deconvolution of low, medium, and high volatility biogenic secondary organic aerosol, Environ. Sci. Technol., 43, 4884-4889, 10.1021/es803676g, 2009.~~

King, S. M., Rosenoern, T., Shilling, J. E., Chen, Q., Wang, Z., Biskos, G., McKinney, K. A., Poschl, U., and Martin, S. T.: Cloud droplet activation of mixed organic-sulfate particles

produced by the photooxidation of isoprene, Atmos. Chem. Phys., 10, 3953-3964, 10.5194/acp-10-3953-2010, 2010.

Kuhn, U., Ganzeveld, L., Thielmann, A., Dindorf, T., Schebeske, G., Welling, M., Sciare, J., Roberts, G., Meixner, F. X., Kesselmeier, J., Lelieveld, J., Kolle, O., Ciccioli, P., Lloyd, J., Trentmann, J., Artaxo, P., and Andreae, M. O.: Impact of Manaus City on the Amazon Green Ocean atmosphere: ozone production, precursor sensitivity and aerosol load, Atmos. Chem. Phys., 10, 9251-9282, 10.5194/acp-10-9251-2010, 2010.

Lambe, A. T., Onasch, T. B., Massoli, P., Croasdale, D. R., Wright, J. P., Ahern, A. T., Williams, L. R., Worsnop, D. R., Brune, W. H., and Davidovits, P.: Laboratory studies of the chemical composition and cloud condensation nuclei (CCN) activity of secondary organic aerosol (SOA) and oxidized primary organic aerosol (OPOA), Atmos. Chem. Phys., 11, 8913-8928, 10.5194/acp-11-8913-2011, 2011.

Lim, Y. B., Tan, Y., Perri, M. J., Seitzinger, S. P., and Turpin, B. J.: Aqueous chemistry and its role in secondary organic aerosol (SOA) formation, Atmos. Chem. Phys., 10, 10521-10539, 10.5194/acp-10-10521-2010, 2010.

Lin, Y. H., Zhang, Z. F., Docherty, K. S., Zhang, H. F., Budisulistiorini, S. H., Rubitschun, C. L., Shaw, S. L., Knipping, E. M., Edgerton, E. S., Kleindienst, T. E., Gold, A., and Surratt, J. D.: Isoprene epoxydiols as precursors to secondary organic aerosol formation: Acid-catalyzed reactive uptake studies with authentic compounds, Environ. Sci. Technol., 46, 250-258, 10.1021/es202554c, 2012.

~~Liu, S., Shilling, J. E., Song, C., Hiranuma, N., Zaveri, R. A., and Russell, L. M.: Hydrolysis of organonitrate functional groups in aerosol particles, Aerosol Sci. Technol., 46, 1359-1369, 10.1080/02786826.2012.716175, 2012.~~

Liu, Y. J., Herdlinger-Blatt, I., McKinney, K. A., and Martin, S. T.: Production of methyl vinyl ketone and methacrolein via the hydroperoxyl pathway of isoprene oxidation, Atmos. Chem. Phys., 13, 5715-5730, 10.5194/acp-13-5715-2013, 2013.

Liu, Y., Kuwata, M., Strick, B. F., Geiger, F. M., Thomson, R. J., McKinney, K. A., and Martin, S. T.: Uptake of epoxydiol isomers accounts for half of the particle-phase material produced from isoprene photooxidation via the HO2 pathway, Environ. Sci. Technol., 49, 250-258, 10.1021/es5034298, 2014.

Malm, W. C., Sisler, J. F., Huffman, D., Eldred, R. A., and Cahill, T. A.: Spatial and seasonal trends in particle concentration and optical extinction in the united states, J. Geophys. Res., 99, 1347-1370, 1994.

Martin, S. T., Andreae, M. O., Artaxo, P., Baumgardner, D., Chen, Q., Goldstein, A. H., Guenther, A., Heald, C. L., Mayol-Bracero, O. L., McMurry, P. H., Pauliquevis, T., Poschl, U., Prather, K. A., Roberts, G. C., Saleska, S. R., Dias, M. A. S., Spracklen, D. V., Swietlicki, E., and Trebs, I.: Sources and properties of amazonian aerosol particles, Reviews of Geophysics, 48, Rg2002, 10.1029/2008rg000280, 2010a.

Martin, S. T., Andreae, M. O., Althausen, D., Artaxo, P., Baars, H., Borrmann, S., Chen, Q., Farmer, D. K., Guenther, A., Gunthe, S. S., Jimenez, J. L., Karl, T., Longo, K., Manzi, A., Muller, T., Pauliquevis, T., Petters, M. D., Prenni, A. J., Poschl, U., Rizzo, L. V., Schneider, J., Smith, J. N., Swietlicki, E., Tota, J., Wang, J., Wiedensohler, A., and Zorn, S. R.: An overview of the Amazonian Aerosol Characterization Experiment 2008 (AMAZE-08), Atmos. Chem. Phys., 10, 11415-11438, 10.5194/acp-10-11415-2010, 2010b.

Matthew, B. M., Middlebrook, A. M., and Onasch, T. B.: Collection efficiencies in an Aerodyne aerosol mass spectrometer as a function of particle phase for laboratory generated aerosols, Aerosol Sci. Technol., 42, 884-898, 10.1080/02786820802356797, 2008.

~~Middlebrook, A. M., Bahreini, R., Jimenez, J. L., and Canagaratna, M. R.: Evaluation of composition-dependent collection efficiencies for the Aerodyne aerosol mass spectrometer using field data, Aerosol Sci. Technol., 46, 258-271, 10.1080/02786826.2011.620041, 2012.~~

Ng, N. L., Canagaratna, M. R., Zhang, Q., Jimenez, J. L., Tian, J., Ulbrich, I. M., Kroll, J. H., Docherty, K. S., Chhabra, P. S., Bahreini, R., Murphy, S. M., Seinfeld, J. H., Hildebrandt, L., Donahue, N. M., DeCarlo, P. F., Lanz, V. A., Prevot, A. S. H., Dinar, E., Rudich, Y., and Worsnop, D. R.: Organic aerosol components observed in Northern Hemispheric datasets from Aerosol Mass Spectrometry, Atmos. Chem. Phys., 10, 4625-4641, 10.5194/acp-10-4625-2010, 2010.

Ng, N. L., Canagaratna, M. R., Jimenez, J. L., Chhabra, P. S., Seinfeld, J. H., and Worsnop, D. R.: Changes in organic aerosol composition with aging inferred from aerosol mass spectra, Atmos. Chem. Phys., 11, 6465-6474, 10.5194/acp-11-6465-2011, 2011.

Nguyen, T. B., Coggon, M. M., Bates, K. H., Zhang, X., Schwantes, R. H., Schilling, K. A., Loza, C. L., Flagan, R. C., Wennberg, P. O., and Seinfeld, J. H.: Organic aerosol formation from the reactive uptake of isoprene epoxydiols (IEPOX) onto non-acidified inorganic seeds, Atmos. Chem. Phys., 14, 3497-3510, 10.5194/acp-14-3497-2014, 2014.

Ortega, A. M., Day, D. A., Cubison, M. J., Brune, W. H., Bon, D., de Gouw, J. A., and Jimenez, J. L.: Secondary organic aerosol formation and primary organic aerosol oxidation from biomass burning smoke in a flow reactor during FLAME-3, Atmos. Chem. Phys., 13, 11551-11571, 10.5194/acp-13-11551-2013, 2013.

Paatero, P., and Tapper, U.: Positive matrix factorization - a nonnegative factor model with optimal utilization of error-estimates of data values, Environmetrics, 5, 111-126, 10.1002/env.3170050203, 1994.

Pankow, J. F.: An absorption-model of the gas aerosol partitioning involved in the formation of secondary organic aerosol, Atmos. Environ., 28, 189-193, 1994.

Petzold, A., Kramer, H., and Schonlinner, M.: Continuous measurement of atmospheric black carbon using a multi-angle absorption photometer, Environmental Science and Pollution Research, 4, 78-82, 2002.

Pöhlker, C., Wiedemann, K. T., Sinha, B., Shiraiwa, M., Gunthe, S. S., Smith, M., Su, H., Artaxo, P., Chen, Q., Cheng, Y. F., Elbert, W., Gilles, M. K., Kilcoyne, A. L. D., Moffet, R. C., Weigand, M., Martin, S. T., Poeschl, U., and Andreae, M. O.: Biogenic potassium salt particles as seeds for secondary organic aerosol in the Amazon, Science, 337, 1075-1078, 10.1126/science.1223264, 2012.

Pöschl, U., Martin, S. T., Sinha, B., Chen, Q., Gunthe, S. S., Huffman, J. A., Borrmann, S., Farmer, D. K., Garland, R. M., Helas, G., Jimenez, J. L., King, S. M., Manzi, A., Mikhailov, E., Pauliquevis, T., Petters, M. D., Prenni, A. J., Roldin, P., Rose, D., Schneider, J., Su, H., Zorn, S. R., Artaxo, P., and Andreae, M. O.: Rainforest aerosols as biogenic nuclei of clouds and precipitation in the Amazon, Science, 329, 1513-1516, 10.1126/science.1191056, 2010.

Prenni, A. J., Petters, M. D., Kreidenweis, S. M., Heald, C. L., Martin, S. T., Artaxo, P., Garland, R. M., Wollny, A. G., and Poschl, U.: Relative roles of biogenic emissions and Saharan dust as ice nuclei in the Amazon basin, Nature Geoscience, 2, 401-404, Doi 10.1038/Ngeo517, 2009.

Rizzo, L. V., Artaxo, P., Muller, T., Wiedensohler, A., Paixao, M., Cirino, G. G., Arana, A., Swietlicki, E., Roldin, P., Fors, E. O., Wiedemann, K. T., Leal, L. S. M., and Kulmala, M.: Long term measurements of aerosol optical properties at a primary forest site in Amazonia, Atmos. Chem. Phys., 13, 2391-2413, 10.5194/acp-13-2391-2013, 2013.

Robinson, N. H., Hamilton, J. F., Allan, J. D., Langford, B., Oram, D. E., Chen, Q., Docherty, K., Farmer, D. K., Jimenez, J. L., Ward, M. W., Hewitt, C. N., Barley, M. H., Jenkin, M. E., Rickard, A. R., Martin, S. T., McFiggans, G., and Coe, H.: Evidence for a significant proportion of secondary organic aerosol from isoprene above a maritime tropical forest, Atmos. Chem. Phys., 11, 1039-1050, 10.5194/acp-11-1039-2011, 2011.

Schneider, J., Freutel, F., Zorn, S. R., Chen, Q., Farmer, D. K., Jimenez, J. L., Martin, S. T., Artaxo, P., Wiedensohler, A., and Borrmann, S.: Mass- spectrometric identification of primary biological particle markers and application to pristine submicron aerosol measurements in Amazonia, Atmos. Chem. Phys., 11, 11415-11429, 10.5194/acp-11-11415-2011, 2011.

Shilling, J. E., Chen, Q., King, S. M., Rosenoern, T., Kroll, J. H., Worsnop, D. R., DeCarlo, P. F., Aiken, A. C., Sueper, D., Jimenez, J. L., and Martin, S. T.: Loading-dependent elemental composition of α-pinene SOA particles, Atmos. Chem. Phys., 9, 771-782, 10.5194/acp-9-771-2009, 2009.

Slowik, J. G., Brook, J., Chang, R. Y. W., Evans, G. J., Hayden, K., Jeong, C. H., Li, S. M., Liggio, J., Liu, P. S. K., McGuire, M., Mihele, C., Sjostedt, S., Vlasenko, A., and Abbatt, J. P. D.: Photochemical processing of organic aerosol at nearby continental sites: contrast between urban plumes and regional aerosol, Atmos. Chem. Phys., 11, 2991-3006, DOI 10.5194/acp-11-2991-2011, 2011.

Surratt, J. D., Chan, A. W. H., Eddingsaas, N. C., Chan, M. N., Loza, C. L., Kwan, A. J., Hersey, S. P., Flagan, R. C., Wennberg, P. O., and Seinfeld, J. H.: Reactive intermediates revealed in secondary organic aerosol formation from isoprene, Proc. Natl. Acad. Sci. U. S. A., 107, 6640-6645, 10.1073/pnas.0911114107, 2010.

Talbot, R. W., Andreae, M. O., Andreae, T. W., and Harriss, R. C.: Regional aerosol chemistry of the Amazon Basin during the dry season, J. Geophys. Res., 93, 1499-1508, 1988.

Talbot, R. W., Andreae, M. O., Berresheim, H., Artaxo, P., Garstang, M., Harriss, R. C., Beecher, K. M., and Li, S. M.: Aerosol chemistry during the wet season in central amazonia: The influence of long-range transport, J. Geophys. Res., 95, 16955-16969, 1990.

Trebs, I., Metzger, S., Meixner, F. X., Helas, G. N., Hoffer, A., Rudich, Y., Falkovich, A. H., Moura, M. A. L., da Silva, R. S., Artaxo, P., Slanina, J., and Andreae, M. O.: The NH_4^+-NO_3^--Cl^--SO_4^{2-}-H_2O aerosol system and its gas phase precursors at a pasture site in the Amazon Basin: How relevant are mineral cations and soluble organic acids?, J. Geophys. Res., 110, D07303, 10.1029/2004JD005478, 2005.

Ulbrich, I. M., Canagaratna, M. R., Zhang, Q., Worsnop, D. R., and Jimenez, J. L.: Interpretation of organic components from Positive Matrix Factorization of aerosol mass spectrometric data, Atmos. Chem. Phys., 9, 2891-2918, 2009.

Vaden, T. D., Imre, D., Beranek, J., Shrivastava, M., and Zelenyuk, A.: Evaporation kinetics and phase of laboratory and ambient secondary organic aerosol, Proc. Natl. Acad. Sci. U. S. A., 108, 2190-2195, 10.1073/pnas.1013391108, 2011.

Zhang, Q., Alfarra, M. R., Worsnop, D. R., Allan, J. D., Coe, H., Canagaratna, M. R., and Jimenez, J. L.: Deconvolution and quantification of hydrocarbon-like and oxygenated organic aerosols based on aerosol mass spectrometry, Environ. Sci. Technol., 39, 4938-4952, 10.1021/es048568l, 2005.

Zhang, Q., Jimenez, J. L., Canagaratna, M. R., Ulbrich, I. M., Ng, N. L., Worsnop, D. R., and Sun, Y. L.: Understanding atmospheric organic aerosols via factor analysis of aerosol mass spectrometry: a review, Anal. Bioanal. Chem., 401, 3045-3067, 10.1007/s00216-011-5355-y, 2011.

List of Figures

The NO_x concentration was measured as < 1 ppbv during these experiments and was estimated later as < 70 ppt for typical operating of the HEC (Liu et al., 2013). The relative intensities of ions having $m/z \geq 65$ were multiplied by 10. The intensities at each m/z represent three experiments that were performed at different SOM particle mass concentrations. A single intensity bar is color-coded by the contribution of different ion families (i.e., fragments containing C, H, O, or N for subscripts of x, y, z, $i \geq 1$) as determined from analysis of the high-resolution spectra (Shilling et al., 2009). The relative intensities of the $H_yO_i^+$ family were derived from the intensity of CO_2^+ based on calibrations described in Chen et al. (2011).

Field Code Changed

Figure 5. Statistical factors HOA, OOA-1, OOA-2, and OOA-3 identified by PMF analysis. The relative intensities of ions having $m/z \geq 65$ were multiplied by 10.

Figure 6. Time series of ~~mass concentrations~~the loadings for the ~~statistical~~ factors HOA, OOA-1, OOA-2, and OOA-3 (left axes; dots) and time series of the concentrations of tracer species, including NO_x, CO, AMS chloride, AMS potassium, aethalometer black-carbon, ~~methyl vinyl ketone~~MVK + ~~methacrolein~~MACR, isoprene, monoterpenes, and sesquiterpenes (right axes; lines). The BVOCs were measured by PTR-MS (Karl et al., 2009).

Figure 7. Comparison of the OOA-3 factor to a synthetic mass spectrum obtained from a linear combination of the mass spectra of laboratory-generated biogenic SOM (30% α-pinene-derived SOM, 20% β-caryophylene-derived SOM, and 50% isoprene-derived SOM at mass concentrations of 0.4 to 0.7 μg m^{-3})~~High-resolution mass spectra of secondary organic material produced in the Harvard Environmental Chamber by the oxidation of biogenic volatile organic compounds for < 1 ppbv NO_x. For isoprene~~

~~photooxidation, the relative intensities of ions having *m/z* > 63 were multiplied by 10. The intensity at each unit mass resolution is color coded by the contribution of different ion families, as determined from analysis of the high resolution spectra (Shilling et al., 2009). The relative intensities of the OH family were derived from the intensity of CO_2^+ based on calibrations described in Chen et al. (2011).~~

Figure 8. Campaign-average ~~D~~diel profiles of the ~~campaign average mass concentrations~~loadings of the ~~statistical~~ factors HOA, OOA-1, OOA-2, and OOA-3.

Figure 9. (top) Mass-diameter distributions measured by the AMS and the daytime wind rose for the two time periods shown in the bottom panel. (upper bottom) Time series of daily mean temperature measured at the top of the measurement tower TT34. (lower bottom) Time series of the fractional contribution by each of the four statistical factors identified by PMF analysis ~~to the submicron organic particle mass concentrations.~~(left axes) and the rain counts (right axes). Two case periods that differ significantly in the fractional contribution of PMF factors are selected.

~~**Figure 9.** Processes depicted for the wet season concerning the production and further reactions of secondary organic material in the submicron size fraction of the Amazonian particle population.~~

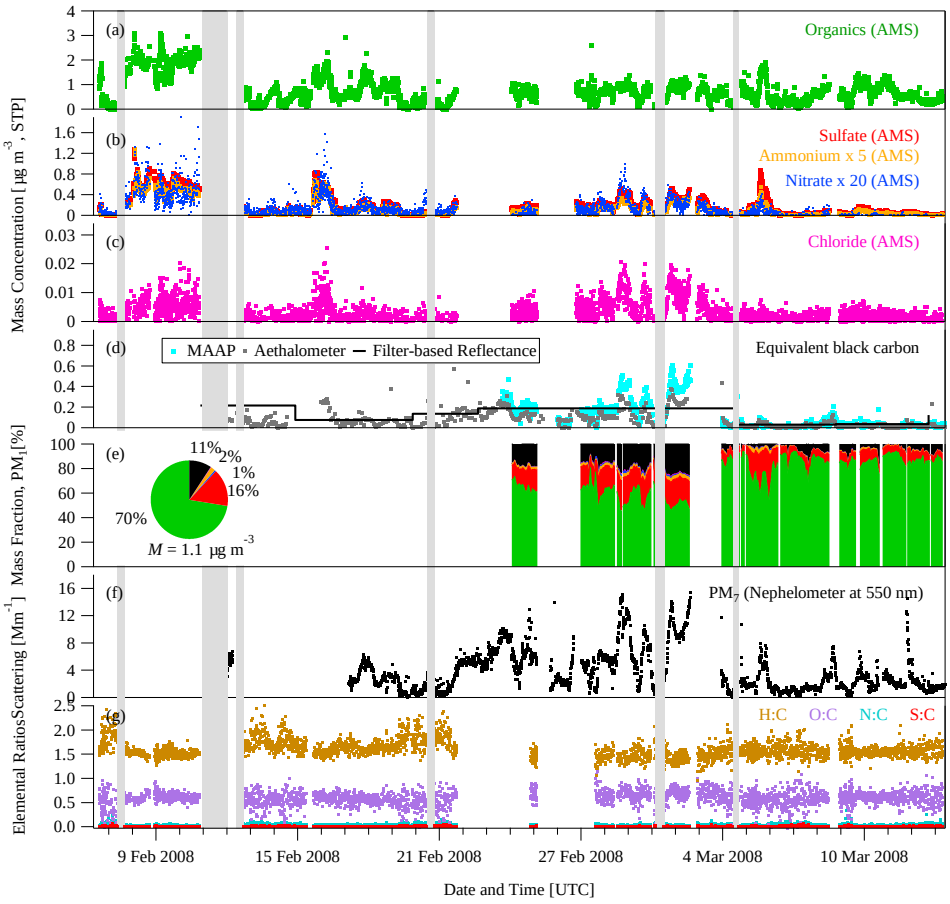
(a)
Organics (AMS)
(b)
Sulfate (AMS)
Ammonium x 5 (AMS)
Nitrate x 20 (AMS)
(c)
Chloride (AMS)
(d)
MAAP
Aethalometer
Filter-based Reflectance
Equivalent black carbon
(e)
11%
2%
1%
16%
70%
M = 1.1 µg m-3
(f)
PM7 (Nephelometer at 550 nm)
(g)
H:C
O:C
N:C
S:C
Mass Concentration [µg m-3, STP]
Mass Fraction, PM1 [%]
Scattering [Mm-1]
Elemental Ratios
9 Feb 2008
15 Feb 2008
21 Feb 2008
27 Feb 2008
4 Mar 2008
10 Mar 2008
Date and Time [UTC]

Figure 1

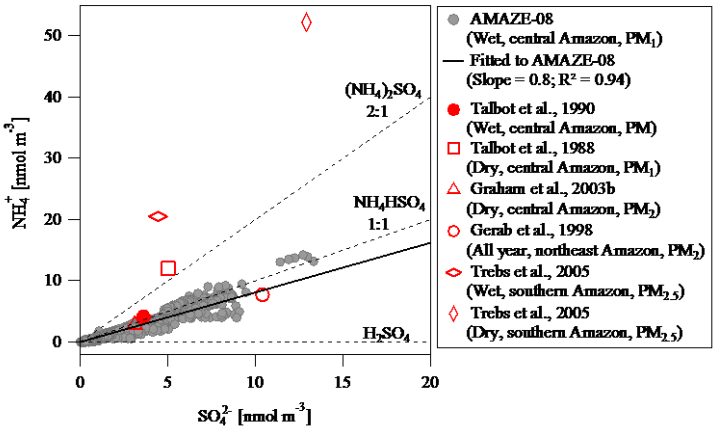
AMAZE-08
(Wet, central Amazon, PM1)
Fitted to AMAZE-08
(Slope = 0.8; R² = 0.94)
Talbot et al., 1990
(Wet, central Amazon, PM)
Talbot et al., 1988
(Dry, central Amazon, PM1)
Graham et al., 2003b
(Dry, central Amazon, PM2)
Gerab et al., 1998
(All year, northeast Amazon, PM2)
Trebs et al., 2005
(Wet, southern Amazon, PM2.5)
Trebs et al., 2005
(Dry, southern Amazon, PM2.5)
(NH4)2SO4
2:1
NH4HSO4
1:1
H2SO4
NH4+ [nmol m-3]
SO42- [nmol m-3]
0
10
20
30
40
50
0
5
10
15
20

Figure 2

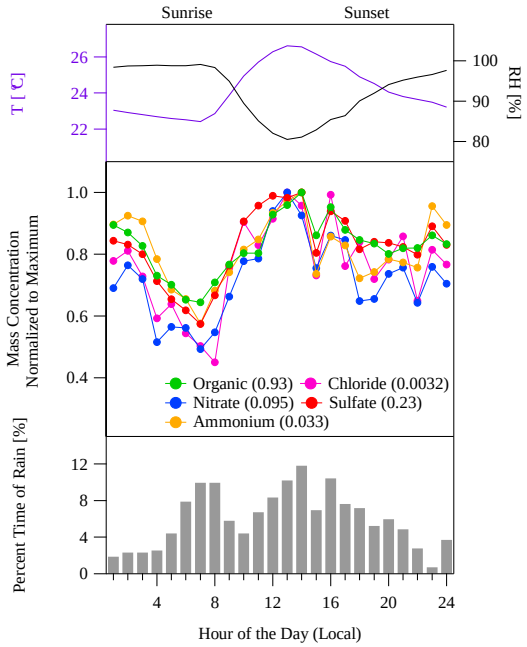
Sunrise
Sunset
T [°C]
26
24
22
RH [%]
100
90
80
Mass Concentration
Normalized to Maximum
1.0
0.8
0.6
0.4
Organic (0.93)
Chloride (0.0032)
Nitrate (0.095)
Sulfate (0.23)
Ammonium (0.033)
Percent Time of Rain [%]
12
8
4
0
4
8
12
16
20
24
Hour of the Day (Local)

Figure 3

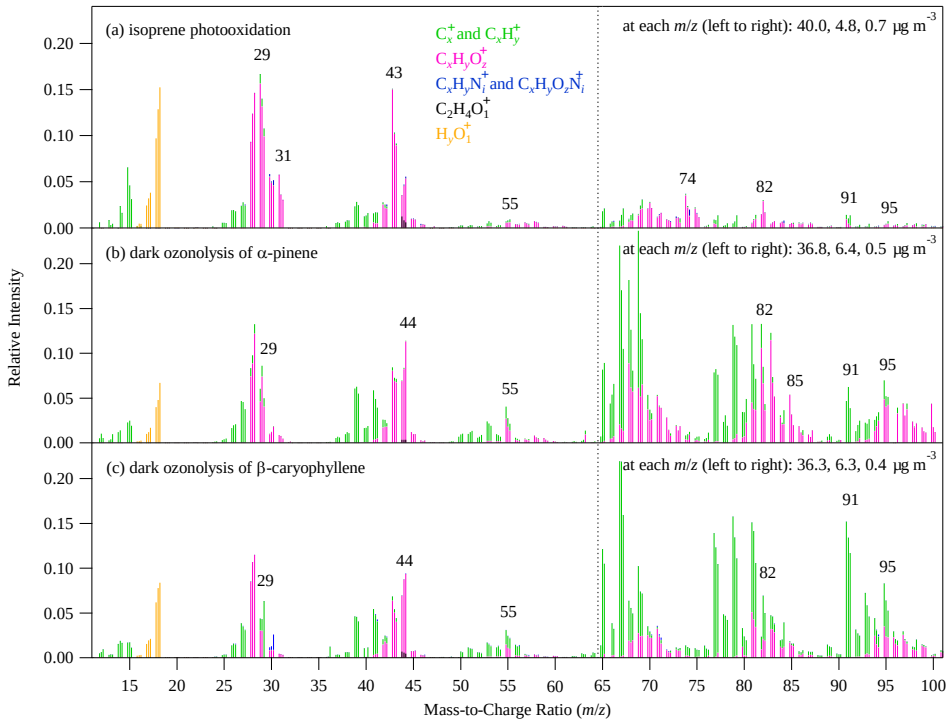
(a) isoprene photooxidation
C_x^+ and $C_xH_y^+$
$C_xH_yO_z^+$
$C_xH_yN_i^+$ and $C_xH_yO_zN_i^+$
$C_2H_4O_1^+$
$H_yO_1^+$
at each m/z (left to right): 40.0, 4.8, 0.7 µg m^{-3}
(b) dark ozonolysis of α-pinene
at each m/z (left to right): 36.8, 6.4, 0.5 µg m^{-3}
(c) dark ozonolysis of β-caryophyllene
at each m/z (left to right): 36.3, 6.3, 0.4 µg m^{-3}
Relative Intensity
Mass-to-Charge Ratio (m/z)

Figure 4

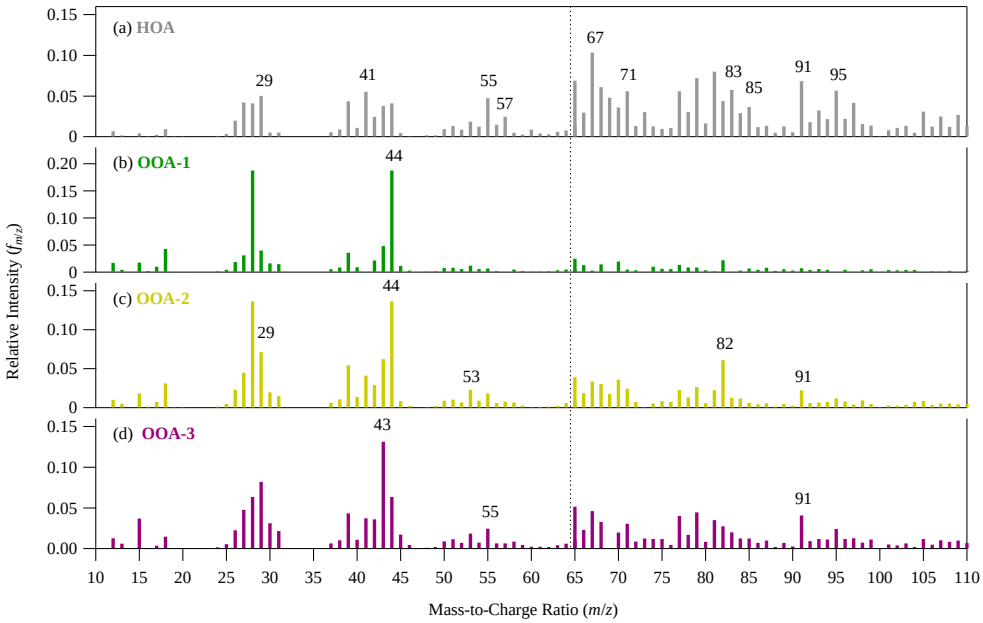
(a) HOA
(b) OOA-1
(c) OOA-2
(d) OOA-3
Relative Intensity ($f_{m/z}$)
Mass-to-Charge Ratio (m/z)

Figure 5

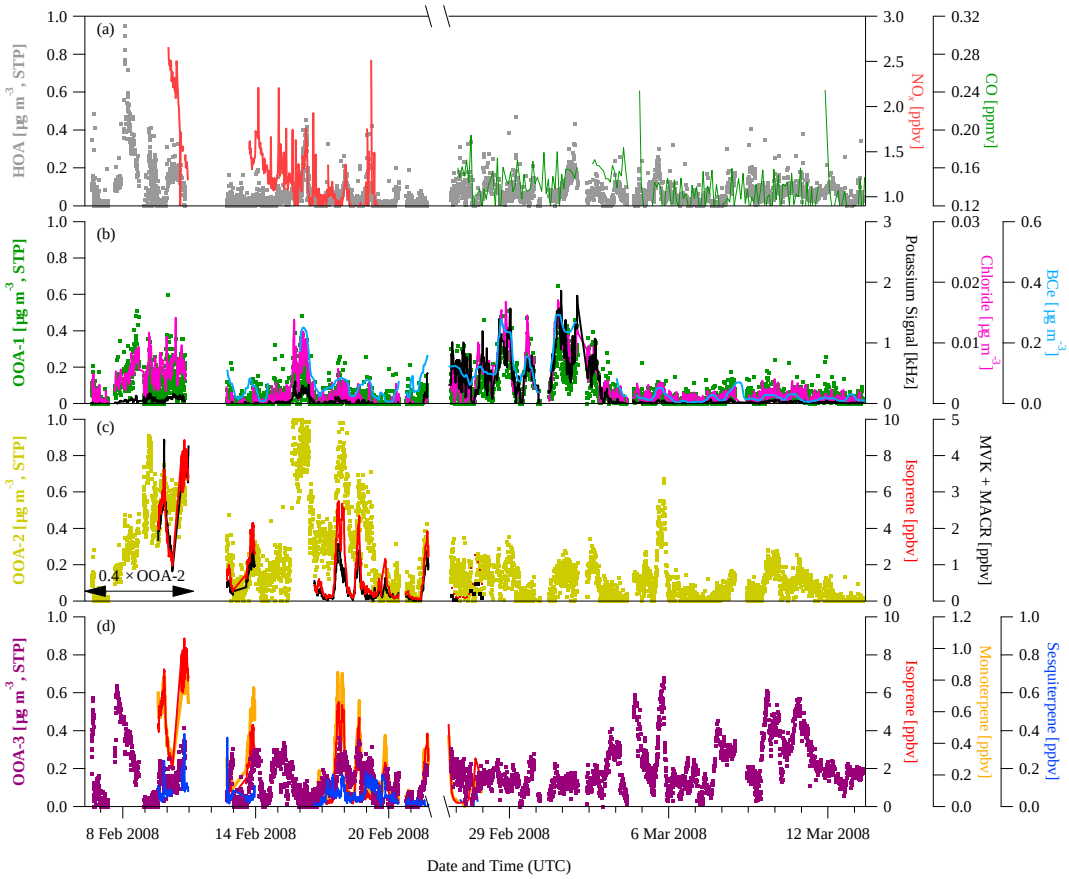
(a)
(b)
(c)
(d)
HOA [μg m-3, STP]
OOA-1 [μg m-3, STP]
OOA-2 [μg m-3, STP]
OOA-3 [μg m-3, STP]
NOx [ppbv]
CO [ppmv]
Potassium Signal [kHz]
Chloride [μg m-3]
BCe [μg m-3]
Isoprene [ppbv]
MVK + MACR [ppbv]
Monoterpene [ppbv]
Sesquiterpene [ppbv]
0.4 × OOA-2
8 Feb 2008
14 Feb 2008
20 Feb 2008
29 Feb 2008
6 Mar 2008
12 Mar 2008
Date and Time (UTC)

Figure 6

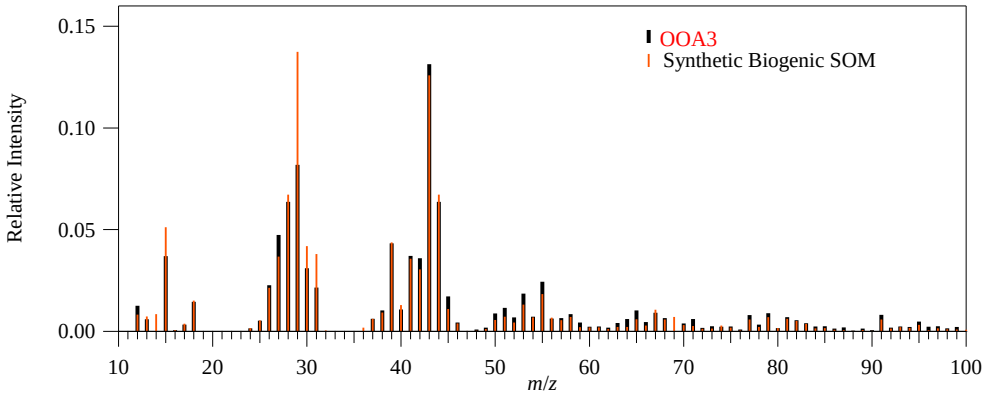
OOA3
Synthetic Biogenic SOM
Relative Intensity
0.15
0.10
0.05
0.00
10
20
30
40
50
60
70
80
90
100
m/z

Figure 7

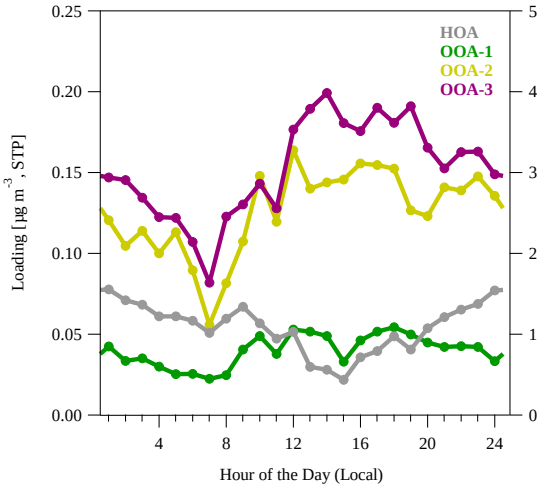
HOA
OOA-1
OOA-2
OOA-3
Loading [μg m -3 , STP]
0.25
0.20
0.15
0.10
0.05
0.00
5
4
3
2
1
0
4
8
12
16
20
24
Hour of the Day (Local)

Figure 8

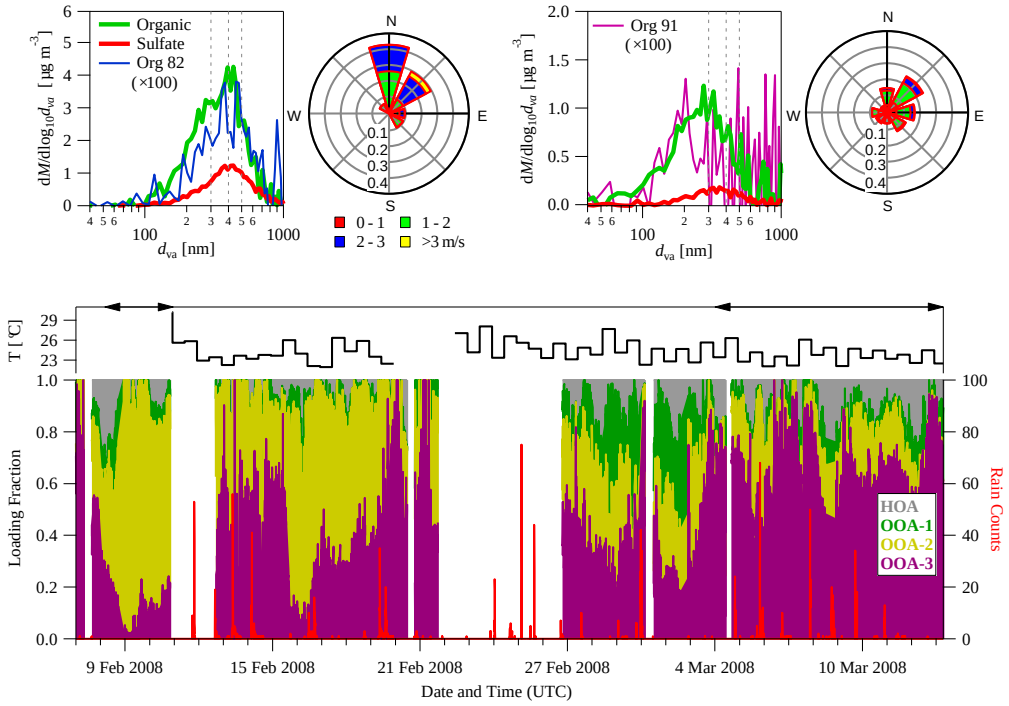
Organic
Sulfate
Org 82
(×100)
Org 91
(×100)
N
S
E
W
0 - 1
1 - 2
2 - 3
>3 m/s
dM/dlog10dva [μg m-3]
dva [nm]
T [℃]
Loading Fraction
Rain Counts
HOA
OOA-1
OOA-2
OOA-3
9 Feb 2008
15 Feb 2008
21 Feb 2008
27 Feb 2008
4 Mar 2008
10 Mar 2008
Date and Time (UTC)

Figure 9

Supplementary Material For

~~Fine-Mode Organic~~Submicron Particle Mass Concentrations and Sources in the Amazonian Wet Season (AMAZE-08)

A. AMS sampling and data processing

~~Chen et al. (2009) and Martin et al. (2010) described the deployment of the AMS. Aerosol particles above the forest canopy were drawn through a stainless steel tube (1/2" OD; 10.9 mm ID) in a turbulent flow of 40 to 80 L min^{-1} to the roof of the instrument container. The flow was then split in three: a 3-m line for filter sampling (20 L min^{-1}), a 2-m line (1/4" OD; 4.8 mm ID) into an Aerodyne high-resolution Aerosol Mass Spectrometer (HR-AMS) (4 L min^{-1}), and a by-pass line. Calculations for a Reynolds number of 5000 to 10000 for the turbulent-flow inlet suggested nearly 100% transmission of particles for diameters of 17 nm to 3.1 μm. The flow in the AMS sampling line passed through a Nafion dryer just prior to entering the instrument container. The sampling RH measured at the AMS inlet ranged from 40% to 70%. Sampling temperature and pressure were also measured inline prior to entering the AMS. A second AMS operated by MPI-C sampled on a laminar-flow line (20 to 35% RH). The major results reported in this paper were confirmed by co-analysis of the MPI-C data set (Schneider et al., 2011).~~

Chen et al. (2009) described the AMS sampling and data processing. Additional details are provided herein. ~~The AMS data were saved in 150-s intervals in alternating medium- (V) and high-resolution (W) modes. For the V-mode, the instrument was operated in "mass spectrum" and "particle-time-of-flight" submodes for equal time periods. The spectra were analyzed using the software toolkits Sequential Igor Data Retrieval (SQUIRREL), Peak Integration by Key Analysis (PIKA), and Analytic Procedure for Elemental Separation (APES).~~ Standard relative

ionization efficiencies (RIE) were used in the analysis, including 1.1 for nitrate, 1.2 for sulfate, 1.4 for organic molecules, 4.0 for ammonium, 1.3 for chloride, and 2.0 for water (DeCarlo et al., 2006; Mensah et al., 2011).

~~Several updates were made to the fragmentation table (Allan et al., 2004). Specifically, the fragmentation coefficients at *m/z* 16, 17, 18, 29, 30, 37, 38, 39, 40, 44, and 46 were adjusted to account for the variability of gas-phase contributions and for the interference of ions having the same nominal *m/z*. The signals of NH_2^+ at *m/z* 16, NH_3^+ at *m/z* 17, NO^+ at *m/z* 30, and NO_2^+ at *m/z* 46 were calculated as time-dependent fractions of the signals at unit resolution. The organic signals of $[CO^+]_{org}$ at *m/z* 28 and $[H_xO^+]_{org}$ at *m/z* 16, 17, and 18 were adjusted using the approach of Aiken et al. (2008). T~~Unlike the analysis in Chen et al. (2009), the organic signals of C_3H^+ at *m/z* 37, $C_3H_2^+$ at *m/z* 38, $C_3H_3^+$ at *m/z* 39, and $C_3H_4^+$ at *m/z* 40, which made up 5-8% of the total organic signal, were calculated time-dependently based on the ratio of them to $C_2H_2^+$ at *m/z* 26. ~~Air contributions (e.g., $^{15}NN^+$ at *m/z* 29) were subtracted as a constant fraction of the N_2^+ signal based on the data recorded with a HEPA filter in-line, with the remaining signal at *m/z* 29 assigned to CHO^+. Variations of the $[CO_2^+]_{air}$ signal at *m/z* 44 were corrected using the measured gas-phase CO_2 concentrations and the data recorded with a HEPA filter in-line. For the periods when there were no gas-phase CO_2 measurements, mean diel CO_2 concentrations were used, which corresponds to 10% error for the organic particle mass concentration of 0.2 μg m^{-3}. For comparison, using only the data recorded with a HEPA filter for this correction caused 20% error at similar mass concentration.~~

~~Mass concentrations were calculated from the V-mode data and were adjusted to standard temperature and pressure (noted as STP; 273 K and 10^5 Pa), which were approximately 10% greater than those at calibration conditions (299.3 K and 100591.7 Pa).~~ In the present study

particle-phase water was not included in the calculations of species mass concentrations.

Occasionally the sampling site was influenced by the exhaust plumes from the site power source, which was a diesel generator located 0.72 km from TT34 and typically downwind. Abrupt increases in AMS-measured sulfate mass concentrations, even greater than the organic concentrations, were indicators of influence by the local pollution source. These pollution events were defined herein excluded from the data sets analyzed ~~herein~~(Fig. 1). Chen et al. (2009) excluded more data by using a broader pollution filter defined by Martin et al. (2010). ~~In the present study particle-phase water was not included in the calculations of species mass concentrations.~~

~~Organosulfate species have been observed both for laboratory-generated biogenic secondary organic particles under acidic conditions as well as for ambient particles sampled in the southeastern USA, Germany, and Hungary. The technique employed in these studies was the analysis of filter samples by electrospray-ionization mass spectrometry coupled to pre-separation by liquid chromatography. In the AMS, the organosulfate species can fragment to organic ions ($C_xH_yO_z^+$), organosulfur ions ($C_xH_yO_zS^+$), and ions with a pattern indistinguishable from inorganic sulfate (e.g., SO_z^+) (Farmer et al., 2010). For the AMAZE-08 data set, signal intensities for $C_xH_yO_zS^+$ ions were not above noise in the collected high-resolution mass spectra. The agreement among AMS, IC, and PIXE sulfate mass concentrations, as well as the absence of organosulfur ions in the high-resolution mass spectra, did not provide evidence for substantial contributions of organosulfate species during AMAZE-08, at least at concentrations above uncertainty levels.~~

The AMS detection limits, calculated as three times the standard deviation of mass concentrations for filtered air obtained at 150-s intervals, were 0.06, 0.02, 0.001, 0.006, 0.002

μg m^{-3} for organic material, sulfate, ammonium, chloride, and nitrate, respectively. The AMS is capable of focusing particles with 30-1000 nm with size-dependent particle transmission efficiency (Liu et al., 2007). As described in Gunthe et al. (2009), we operated the AMS at sampling pressures of 867–907 hPa. Under these conditions, the transmission efficiency is close to 100% for particles with vacuum aerodynamic diameter d_{va} of 100–400 nm and is greater than 20% for particles with d_{va} of 50-1000 nm. For organic measurements, the estimated uncertainty is 30% at concentrations of 1 μg m^{-3} to 40% at concentrations of 0.5 μg m^{-3}. It can increase to 100% for low organic concentrations (0.1 μg m^{-3}). For sulfate measurements, the uncertainty is <10% for high concentrations (0.5 μg m^{-3}) and about 40% for low concentrations (0.05 μg m^{-3}).

~~The mass-diameter distributions reported herein for the AMS represented the average of 74 measurements. The distributions were selected for time periods having nearly identical mass concentrations of sulfate. For comparison, nephelometer data at 550 nm were averaged for the same time periods. The mass-diameter distributions were multiplied by diameter-dependent mass extinction efficiencies (m^2 g^{-1}) to estimate light scattering coefficients. The mass extinction efficiencies were calculated at 550 nm using Mie theory for a refractive index of 1.42 – 0.006 i (Guyon et al., 2003). An agreement was found between calculated and measured aerosol scattering coefficients, particularly for periods free of influence of long-range advection of mineral dust (see further in Sect. B and Fig. S2). Comparisons were also made between the AMS mass-diameter distributions and volume-diameter distributions measured by a Scanning Mobility Particle Sizer (Lund SMPS), consisting of a differential mobility analyzer attached to a condensation particle counter (Roldin, 2008). The combined data sets were used to estimate the particle effective density ρ_{eff} (kg m^{-3}) based on an in-common mode diameter (Katrib et al., 2005) and the organic density ρ_{org} (see further in Sect. B and Fig. S3). The analysis obtained ρ_{eff} of~~

~~1390 ± 150 kg m^{-3} and ρ_{org} of 1270 ± 110 kg m^{-3} for the AMAZE-08 data set.~~

Atomic ratios of oxygen-to-carbon (O:C), hydrogen-to-carbon (H:C), and nitrogen-to-carbon (N:C), as well as the mass ratios of organic material to organic carbon (OM:OC), were calculated from the W-mode data following previously described methods (Aiken et al., 2008). A recent study shows that organic aerosol with mixed keto-, hydroxyl-, and acid-functionalities readily undergo thermally-induced dehydration and decarboxylation on the AMS vaporizer (Canagaratna et al., 2015). Such dehydration and decarboxylation can lead much greater $(CO^+)_{org}$:$(CO_2^+)_{org}$ and $(H_2O^+)_{org}$:$(CO_2^+)_{org}$ ratios than the ones that have been empirically used in the "general" elemental analysis described by Aiken et al. (2008). A correction of 34% increase in O:C and 17% increase in H:C was applied based on ~~Canagaratna's~~the correction formula reported by Canagaratna et al. (2015)~~(2013)~~.

In the AMS, the organosulfate species can fragment to organic ions ($C_xH_yO_z^+$), organosulfur ions ($C_xH_yO_zS^+$), and ions with a pattern indistinguishable from inorganic sulfate (e.g., SO_2^+) (Farmer et al., 2010). Similarly, the organonitrate species also fragment to the NO_x^+ ions and are detected as inorganic nitrate by the AMS. ~~The contributions of organonitrates and organosulfates, detected as inorganic nitrate or sulfate ions, to the elemental ratios were negligible because their low mass concentrations.~~For the AMAZE-08 data set, signal intensities for $C_xH_yO_zS^+$ ions were not above noise in the collected high-resolution mass spectra. The agreement among AMS, IC, and PIXE sulfate mass concentrations, as well as the absence of organosulfur ions in the high-resolution mass spectra, ~~did not provide evidence for substantial contributions of organosulfate species during AMAZE-08~~suggest minimal mass concentration of organosulfate species, at least at concentrations above uncertainty levels. Nitrate had a campaign-average concentration of 7 ± 2 ng m^{-3}. This value was greater than the average fine-

mode concentration of 4 ± 1 ng m^{-3} measured by IC. As a test against possible significance of organonitrate species to the results of the present study, a limiting assumption that assigns all AMS-measured nitrate to organonitrate increases the average O:C ratio by <0.01 for the elemental analysis and corresponds to a maximum of 5% contribution of organonitrates to the total organic particle mass concentration for an assumed molecular weight of 360 g mol^{-1} (Chen et al., 2011). The low mass concentration of particle-phase organonitrates is expected because of the low prevailing NO_x concentrations and humid environment (Day et al., 2010; Liu et al., 2012).

B. Other concurrent measurements and comparisons among measurements

Instruments making measurements during AMAZE-08 at the TT34 site are listed in Martin et al. (2010). The size distribution of particles between 0.010 and 0.48 μm (mobility diameter) was measured every 5 min by a Scanning Mobility Particle Sizer (Lund SMPS) (Roldin, 2008). Particle volume concentrations were calculated from the SMPS size distributions for an assumption of spherical particles. The total number concentration for particles greater than 0.010 μm was measured every 3 s by a Condensation Particle Counter (CPC, TSI 3010). Particle scattering coefficients at multiple wavelengths were measured every 1 min by a nephelometer (TSI 3563) and averaged to 10 min. The light absorption at 637 nm of deposited particles was measured every 1 min by the Multiangle Absorption Photometer (MAAP, Thermo 5012). These several instruments sampled through a laminar-flow line (i.e., separate sampling from the AMS line) that was characterized by lower and upper limits of transmission for particle diameters of 0.004 and 7 μm, respectively (Martin et al., 2010).

Several particle filter samples were collected (Artaxo et al., 2013). Total-particle filters (TPF; PM_3) were collected in-line with the turbulent inlet used by the AMS. Stacked filter units

(SFU) were installed separately at 10 m to sample fine- (PM_2) and coarse-mode particles (PM_{2-10}). The two types of filters show reasonable agreement on the particle mass concentration (Table S2). The fine-mode data from SFU are reported herein. Filter samples were analyzed by ion chromatography (IC) for water-soluble ionic components, including sulfate, nitrate, and ammonium, among other components. The filters were also analyzed by particle-induced X-ray emission (PIXE) for elemental composition. Concentrations were adjusted to STP conditions.

The AMS data can be compared to other concurrent measurements of AMAZE-08. The mass ratio of NR-PM_1 measured by the AMS to PM_2 by filter assays was 0.65 as a campaign average (Table S2). The ratio was less than unity because PM_2 included contributions by black carbon and mineral dust (Sect. 3.1) as well as organic material in the diameter range of 1 to 2 μm (Pöschl et al., 2010). Particle mass-diameter distributions obtained from gravimetric analysis of stages of a Multi-Orifice Uniform Deposit Impactor (MOUDI) showed that an average of 30% of the particle mass concentration was associated with diameter range from 1 to 2 μm (cf. Fig. 16 in Martin et al. (2010)).

Figure S6a shows a line of slope m of 1.24 and correlation R^2 of 0.81 in a scatter plot between the AMS-calculated and the SMPS-derived particle volume concentrations. Figure S6b shows the scatter plot of the number concentrations obtained by integrating the SMPS measurements and those directly measured by the CPC. The slope of 0.6 (R^2 = 0.90) indicates that the CPC measured more particles than the corresponding SMPS-derived quantity. The SMPS bias to particle undercounting can explain $m > 1$ in the scatter plot of Fig. S6a. The scatter plot between sulfate particle mass concentrations measured by the AMS and those measured by IC analysis of the filters is fit by a line of m = 0.90 and R^2 = 0.50 (Fig. S6c).

The combined AMS and SMPS data sets were used to estimate the particle effective

density ρ_{eff} (kg m^{-3}) based on an in-common mode diameter (Katrib et al., 2005). For nonporous spherical particles, material density ρ has the same values as ρ_{eff}, and this condition was assumed to hold in the performed data analysis. The organic material density ρ_{org} was then derived by assuming volume additivity and by using ρ_{inorg} of 1780 kg m^{-3} as ammonium bisulfate for the inorganic components. The estimated campaign-average value of ρ_{eff} for submicron Amazonian particles is 1390 $\pm$ 150 kg m^{-3}. Figure S7 shows one example of the mass-diameter distribution measured by the AMS compared to that derived from the SMPS measurements. Assuming that the chemical components either do not mix or alternatively have a numerically small excess volume of mixing, we can derive ρ_{org} of 1270 $\pm$ 110 kg m^{-3} based on the campaign-average chemical composition and a density of 1770 kg m^{-3} for all inorganic components (Cross et al., 2007). The value of ρ_{org} is consistent with the density of 1200-1500 kg m^{-3} observed for laboratory-generated biogenic secondary organic material (Bahreini et al., 2005; Shilling et al., 2009; Chen et al., 2012).

Figure S6d shows the linear regression of the light scattering derived from the AMS (PM_1) and the nephelometer measurements (PM_7), all for 550-nm wavelength. In total, 74 time periods having nearly identical mass concentrations of sulfate were selected to obtain the averaged particle mass-diameter distributions measured by the AMS. For comparison, nephelometer data at 550 nm were averaged for the same time periods. The mass-diameter distributions were multiplied by diameter-dependent mass extinction efficiencies (m^2 g^{-1}) to estimate light scattering coefficients. The mass extinction efficiencies were calculated at 550 nm using Mie theory for a refractive index of 1.42 - 0.006 *I* (Guyon et al., 2003). An agreement was found between calculated and measured aerosol scattering coefficients, particularly for periods free of influence of long-range advection of mineral dust. During the period of 22 February to 3 March

2008, the ratio of the AMS volume concentration to the nephelometer scattering is high (Fig. S8b). Elevated mass concentrations of mineral dust are observed by the lidar measurements (Baars et al., 2011) and the filter-based PIXE analysis (Prenni et al., 2009). ~~Furthermore, l~~Local wind and Hysplit back trajectories showed a Manaus plume on March 1, 2008. The elevated scattering is, therefore, plausibly a combination of African advection and Manaus plume influence although the coarse-mode contribution from mineral dust is the major driven force of the a weak correlation (R^2 = 0.21) between the nephelometer and AMS dataset. In contrast, a strong correlation (m = 0.62; R^2 = 0.82) of the two data sets is shown for other periods, suggesting a dominant contribution of the non-refractory submicron volume to the total particle scattering. This non-refractory submicron volume is mainly organic material. The scattering coefficients related to the submicron organic material can go up to 6 Mm^{-1} at 550 nm.

C. Positive-Matrix Factorization

Positive-matrix factorization (PMF) is a receptor-based model using a weighted least squares method to identify patterns in data. With caveats, it can be a useful tool to derive the source profiles of organic components from AMS data sets (Ulbrich et al., 2009). In this study, the PMF analysis was conducted on the V-mode organic UMR spectra (m/z 12 to 220). The spectra were analyzed using the SQUIRREL tookit. Prior to PMF analysis, the data set was pre-filtered to remove inorganic contributions, and the analysis was carried out only on the residual data set of the organic component. Fifteen m/z values were omitted because of the absence of organic ions. The time periods associated with random spikes, abrupt increase in sulfate mass concentrations, and little temporal variation caused by the instrument adjustments (Fig. 1) were removed. The error values were calculated using the method described by Ulbrich et al. (2009). Fragments having signal-to-noise ratio less than 2 and fragments set proportionally to m/z 44

were downweighted by increasing their error estimates (Ulbrich et al., 2009). C_xF_y ions contributed significantly to the signals at *m*/*z* 69, 119, 131, 169, 181, and 219, indicating the contamination of Fomblin lubricating oil, possibly from instrument pumps at the site (Cross et al., 2009). These signals appeared always as one statistical factor, with a spiky time series for the loading of that factor. These fragments were downgraded by increasing their error by 100 times. The PMF analysis was conducted with (1) different model error and (2) different seed number. The former was introduced to add modeling uncertainty to the instrumental uncertainty, reflecting the errors that may occur when the true factors do not have constant mass spectra. The latter represents the pseudo-random starting values. Unless otherwise noted, results are presented for both the model error and the seed number of zero. PMF produces a fit to the data, which is called a solution. The solution contains a set of factors and concentrations. For AMAZE-08, four statistical factors were identified and labeled as HOA, OOA-1, OOA-2, and OOA-3 (Fig. 4). The four factors HOA, OOA-1, OOA-2, and OOA-3 respectively accounted for 2%, 18%, 14%, and 66% of the variance in the data matrix, implying a residual variance of <1%.

Number p of factors

Several mathematical metrics were used to set the number *p* of factors. The ratio Q:Q_{exp} of the sum of the squares of the uncertainty-weighted residuals to the expected values decreased by 16%, 8%, 3%, and 3% for *p* increasing from 2 to 5. Three or more factors therefore significantly account for the variance of data. The residual was 1% for $p = 2$ or 3 and < 0.3% for $p = 4$. Structure in the residual was significantly reduced by increasing from *p* of 3 to 4 (Fig. S9). For these reasons, a choice of $p = 4$ was made for the PMF analysis.

The choice of $p = 4$ was also evaluated with respect to factor similarity and correlations of the time series of the factors. Increasing the *p* from 4 to 5 resulted in strongly correlation (R^2 =

0.96) among the factors (Fig. S10). No sufficient information from the correlations with other tracers exists to anticipate this correlation; correlation among factors for *p* of 5 is believed to arise from a splitting of real factors.

Rotational ambiguity of solutions (*FPEAK*).

FPEAK is the rotational parameter. For simplicity, *FPEAK* = 0 was used as the best representation of the PMF solution for this study. The PMF solution was evaluated for uniqueness under linear transformations ("rotations") by varying the *FPEAK* parameter (Ulbrich et al., 2009). Solutions with *FPEAK* between -0.6 and 0.6 increase Q:Q_{exp} by 1%. Figure S11 shows the time series of factor concentrations over this *FPEAK* range. Changes in time series are relatively small compared to the changes in the features of the factors. The largest change is for the HOA factor. This factor accounts for a low fraction of the total signal and hence its features can change without causing a great increase in the residual. The rotational uncertainty causes no conflicts in the interpretation of the PMF factors.

Uncertainty of the solutions.

The results of running the PMF analysis for different pseudo-random starting values (i.e., seeds of 0 to 10) show negligible changes in the factors ($R^2 > 0.999$; $m > 0.995$) and the time series of the concentrations ($R^2 > 0.999$; $m > 0.95$). Testing a "model error" of 5% in the PMF analysis leads to changes in the factor profiles ($R^2 > 0.80$; $m > 0.90$) and in the time series of concentrations ($R^2 > 0.95$; $m > 0.75$) that are close to tolerance.

Quantitative assessment of the uncertainty of the factors is also made by 100 bootstrapping runs (Ulbrich et al., 2009). The results show that the uncertainties in the time series of the concentrations are 15% for the OOA-2 and OOA-3 factors and 30% for the OOA-1 and HOA factors. The uncertainties in the factor spectra are <4% for OOA-2 and OOA-3 and <9%

for OOA-1 and HOA. The mass spectrum of the HOA factor has the largest uncertainty (Fig. S12).

D. Mass spectral markers of biogenic secondary organic material

In the framework of semivolatile partitioning, changes in the chemical composition of secondary organic material with particle-phase organic mass concentration M_{org} are expected: only the least volatile oxidation products can effectively condense to the particle phase at low M_{org} (Donahue et al., 2006). The mass spectra of secondary organic material (SOM) are hence loading-dependent. For the purpose of comparing the mass spectra of chamber data with the AMAZE-08 data, SOM production from the oxidation of a C_5-C_{10}-C_{15} terpene sequence, including the photooxidation of isoprene, the dark ozonolysis of α-pinene, and the dark ozonolysis of β-caryopyhllene, has been studied systematically over a range of M_{org} in the Harvard Environmental Chamber at low NO_x and moderate RH conditions (Chen et al., 2011).

Figure 6 shows the loading-dependent mass spectra of the three types of SOM. The fragmentation pattern extends to higher *m/z* for the increasing carbon skeleton of precursor VOCs. Signals at *m/z* < 60 account for 93-97%, 80-84%, and 71-79% of the total signal intensity for the isoprene, α-pinene, and β-caryophyllene SOM, respectively. For all three types of SOA, the relative intensities of major C_xH_y ions such as CH_3^+ at *m/z* 15, $C_2H_3^+$ at *m/z* 27, $C_3H_3^+$ at *m/z* 39, and $C_3H_5^+$ at *m/z* 41 are typically smaller at lower M_{org}. In contrast, the relative intensity of CO_2^+ at *m/z* 44 increases with decreasing M_{org}. Moreover, the relative intensity of $C_2H_4O^+$ (colored as purple in Fig. 6) increases with increasing M_{org}, accounting for about 10 to 50%, 3 to 5%, and 5 to 10% of the signal at *m/z* 44 for the isoprene, α-pinene, and β-caryophyllenethe SOM, respectively.

The mass spectra of isoprene SOM is consistent with the spectra collected in a batch-

mode chamber experiments under low-NO_x and dry conditions (Chhabra et al., 2010), showing a unique pattern compared to the spectra of the other two SOMs. The spectra of the isoprene SOM are dominated by CHO^+ (*m/z* 29) and $C_2H_3O^+$ (*m/z* 43). The two ions both show a decreasing trend for decreasing M_{org}. The relative intensities of CH_2O^+ at *m/z* 30 and CH_3O^+ at *m/z* 31 are small in the spectra of the α-pinene and β-caryophyllene SOM, and however, are five times greater in the spectra of the isoprene SOM. Moreover, I_{44}:I_{org} has been used as a surrogate of O:C, where $I_{m/z}$ represents the absolute signal intensity at a *m/z* value (Aiken et al., 2008; Ng et al., 2010). Our data show that the isoprene SOM does not follow the empirical relationship between O:C and I_{44}:I_{org} (Fig. S10). Deriving O:C from I_{44}:I_{org} requires careful judgments on the contribution of isoprene SOM.

A general marker for the three biogenic SOM is identified as $C_7H_7^+$ at *m/z* 91 distinct from adjacent ions. The prominent $C_7H_7^+$ companied with a negligible signal of $C_6H_{13}^+$ at *m/z* 85 is also unique for the three biogenic SOA studied in the chamber. In urban environment, ions $C_xH_y^+$ adjacent to $C_7H_7^+$ typically have greater intensities and $C_6H_{13}^+$ has greater relative intensity than $C_7H_7^+$ (cf. Figure 9 in Zhang et al. (2005)). Moreover, $C_5H_6O^+$ at *m/z* 82 is more prominent compared to the adjacent peaks in the spectra of the isoprene SOM than in the spectra of other two types of biogenic SOM. This ion is suggested as a marker for the SOM originated from isoprene (Robinson et al., 2011).

Literature Cited

Aiken, A. C., Decarlo, P. F., Kroll, J. H., Worsnop, D. R., Huffman, J. A., Docherty, K. S., Ulbrich, I. M., Mohr, C., Kimmel, J. R., Sueper, D., Sun, Y., Zhang, Q., Trimborn, A., Northway, M., Ziemann, P. J., Canagaratna, M. R., Onasch, T. B., Alfarra, M. R., Prevot, A. S. H., Dommen, J., Duplissy, J., Metzger, A., Baltensperger, U., and Jimenez, J. L.: O/C and OM/OC ratios of primary, secondary, and ambient organic aerosols with high-resolution time-of-flight aerosol mass spectrometry, Environ. Sci. Technol., 42, 4478-4485, 10.1021/es703009q, 2008.

Artaxo, P., Rizzo, L. V., Brito, J. F., Barbosa, H. M. J., A., A., Sena, E. T., Cirino, G. G., Bastos, W., Martin, S. T., and Andreae, M. O.: Atmospheric aerosols in Amazonia and land use change: from natural biogenic to biomass burning conditions, Faraday Discuss., 165, 1-31, 10.1039/c3fd00052d, 2013.

Baars, H., Ansmann, A., Althausen, D., Engelmann, R., Artaxo, P., Pauliquevis, T., and Souza, R.: Further evidence for significant smoke transport from Africa to Amazonia, Geophys. Res. Lett., 38, L20802, 10.1029/2011GL049200, 2011.

Bahreini, R., Keywood, M. D., Ng, N. L., Varutbangkul, V., Gao, S., Flagan, R. C., Seinfeld, J. H., Worsnop, D. R., and Jimenez, J. L.: Measurements of secondary organic aerosol from oxidation of cycloalkenes, terpenes, and m-xylene using an Aerodyne aerosol mass spectrometer, Environ. Sci. Technol., 39, 5674-5688, 10.1021/es048061a, 2005.

Canagaratna, M. R., Jimenez, J. L., Kroll, J. H., Chen, Q., Kessler, S. H., Massoli, P., Hildebrandt Ruiz, L., Fortner, E., Williams, L. R., Wilson, K. R., Surratt, J. D., Donahue, N. M., Jayne, J. T., and Worsnop, D. R.: Elemental ratio measurements of organic compounds using aerosol mass spectrometry: characterization, improved calibration, and implications, Atmos. Chem. Phys., 15, 253-272, 10.5194/acp-15-253-2015, 2015.

Chen, Q., Farmer, D. K., Schneider, J., Zorn, S. R., Heald, C. L., Karl, T. G., Guenther, A., Allan, J. D., Robinson, N., Coe, H., Kimmel, J. R., Pauliquevis, T., Borrmann, S., Poschl, U., Andreae, M. O., Artaxo, P., Jimenez, J. L., and Martin, S. T.: Mass spectral characterization of submicron biogenic organic particles in the Amazon Basin, Geophys. Res. Lett., 36, L20806, 10.1029/2009gl039880, 2009.

Chen, Q., Liu, Y., Donahue, N. M., Shilling, J. E., and Martin, S. T.: Particle-phase chemistry of secondary organic material: Modeled compared to measured O:C and H:C elemental ratios provide constraints, Environ. Sci. Technol., 45, 4763-4770, 10.1021/es104398s, 2011.

Chen, Q., Li, Y. L., McKinney, K. A., Kuwata, M., and Martin, S. T.: Particle mass yield from β-caryophyllene ozonolysis, Atmos. Chem. Phys., 12, 3165-3179, 10.5194/acp-12-3165-2012, 2012.

Cross, E. S., Slowik, J. G., Davidovits, P., Allan, J. D., Worsnop, D. R., Jayne, J. T., Lewis, D. K., Canagaratna, M., and Onasch, T. B.: Laboratory and ambient particle density determinations using light scattering in conjunction with aerosol mass spectrometry, Aerosol Sci. Technol., 41, 343-359, 10.1080/02786820701199736, 2007.

Cross, E. S., Onasch, T. B., Canagaratna, M., Jayne, J. T., Kimmel, J., Yu, X. Y., Alexander, M. L., Worsnop, D. R., and Davidovits, P.: Single particle characterization using a light scattering module coupled to a time-of-flight aerosol mass spectrometer, Atmos. Chem. Phys., 9, 7769-7793, 2009.

Day, D. A., Liu, S., Russell, L. M., and Ziemann, P. J.: Organonitrate group concentrations in submicron particles with high nitrate and organic fractions in coastal southern California, Atmos. Environ., 44, 1970-1979, 10.1016/j.atmosenv.2010.02.045, 2010.

DeCarlo, P. F., Kimmel, J. R., Trimborn, A., Northway, M. J., Jayne, J. T., Aiken, A. C., Gonin, M., Fuhrer, K., Horvath, T., Docherty, K. S., Worsnop, D. R., and Jimenez, J. L.: Field-deployable, high-resolution, time-of-flight aerosol mass spectrometer, Anal. Chem., 78, 8281-8289, 10.1021/ac061249n, 2006.

Docherty, K. S., Stone, E. A., Ulbrich, I. M., DeCarlo, P. F., Snyder, D. C., Schauer, J. J., Peltier, R. E., Weber, R. J., Murphy, S. M., Seinfeld, J. H., Grover, B. D., Eatough, D. J., and Jimenez, J. L.: Apportionment of primary and secondary organic aerosols in southern California during the 2005 Study of Organic Aerosols in Riverside (SOAR-1), Environ. Sci. Technol., 42, 7655-7662, 10.1021/es8008166, 2008.

Farmer, D. K., Matsunaga, A., Docherty, K. S., Surratt, J. D., Seinfeld, J. H., Ziemann, P. J., and Jimenez, J. L.: Response of an aerosol mass spectrometer to organonitrates and organosulfates and implications for atmospheric chemistry, Proc. Natl. Acad. Sci. U. S. A., 107, 6670-6675, 10.1073/pnas.0912340107, 2010.

Gomez-Gonzalez, Y., Surratt, J. D., Cuyckens, F., Szmigielski, R., Vermeylen, R., Jaoui, M., Lewandowski, M., Offenberg, J. H., Kleindienst, T. E., Edney, E. O., Blockhuys, F., Van Alsenoy, C., Maenhaut, W., and Claeys, M.: Characterization of organosulfates from the photooxidation of isoprene and unsaturated fatty acids in ambient aerosol using liquid chromatography/(-) electrospray ionization mass spectrometry, J. Mass Spectrom., 43, 371-382, 10.1002/jms.1329, 2008.

Gunthe, S. S., King, S. M., Rose, D., Chen, Q., Roldin, P., Farmer, D. K., Jimenez, J. L., Artaxo, P., Andreae, M. O., Martin, S. T., and Pöschl, U.: Cloud condensation nuclei in pristine tropical rainforest air of Amazonia: size-resolved measurements and modeling of atmospheric aerosol composition and CCN activity, Atmos. Chem. Phys., 9, 7551-7575, 10.5194/acp-9-7551-2009, 2009.

Guyon, P., Boucher, O., Graham, B., Beck, J., Mayol-Bracero, O. L., Roberts, G. C., Maenhaut, W., Artaxo, P., and Andreae, M. O.: Refractive index of aerosol particles over the Amazon tropical forest during LBA-EUSTACH 1999, J. Aerosol Sci., 34, 883-907, 10.1016/s0021-8502(03)00052-1, 2003.

Iinuma, Y., Boge, O., Kahnt, A., and Herrmann, H.: Laboratory chamber studies on the formation of organosulfates from reactive uptake of monoterpene oxides, Phys. Chem. Chem. Phys., 11, 7985-7997, 10.1039/b904025k, 2009.

Katrib, Y., Martin, S. T., Rudich, Y., Davidovits, P., Jayne, J. T., and Worsnop, D. R.: Density changes of aerosol particles as a result of chemical reaction, Atmos. Chem. Phys., 5, 275-291, 2005.

Liu, P. S. K., Deng, R., Smith, K. A., Williams, L. R., Jayne, J. T., Canagaratna, M. R., Moore, K., Onasch, T. B., Worsnop, D. R., and Deshler, T.: Transmission efficiency of an aerodynamic focusing lens system: Comparison of model calculations and laboratory measurements for the Aerodyne Aerosol Mass Spectrometer, Aerosol Sci. Technol., 41, 721-733, 10.1080/02786820701422278, 2007.

Liu, S., Shilling, J. E., Song, C., Hiranuma, N., Zaveri, R. A., and Russell, L. M.: Hydrolysis of organonitrate functional groups in aerosol particles, Aerosol Sci. Technol., 46, 1359-1369, 10.1080/02786826.2012.716175, 2012.

Martin, S. T., Andreae, M. O., Althausen, D., Artaxo, P., Baars, H., Borrmann, S., Chen, Q., Farmer, D. K., Guenther, A., Gunthe, S. S., Jimenez, J. L., Karl, T., Longo, K., Manzi, A., Muller, T., Pauliquevis, T., Petters, M. D., Prenni, A. J., Poschl, U., Rizzo, L. V., Schneider, J., Smith, J. N., Swietlicki, E., Tota, J., Wang, J., Wiedensohler, A., and Zorn, S. R.: An overview of the Amazonian Aerosol Characterization Experiment 2008 (AMAZE-08), Atmos. Chem. Phys., 10, 11415-11438, 10.5194/acp-10-11415-2010, 2010.

Mensah, A. A., Buchholz, A., Mentel, T. F., Tillmann, R., and Kiendler-Scharr, A.: Aerosol mass spectrometric measurements of stable crystal hydrates of oxalates and inferred relative ionization efficiency of water, J. Aerosol Sci., 42, 11-19, 10.1016/j.jaerosci.2010.10.003, 2011.

Pöschl, U., Martin, S. T., Sinha, B., Chen, Q., Gunthe, S. S., Huffman, J. A., Borrmann, S., Farmer, D. K., Garland, R. M., Helas, G., Jimenez, J. L., King, S. M., Manzi, A., Mikhailov, E., Pauliquevis, T., Petters, M. D., Prenni, A. J., Roldin, P., Rose, D., Schneider, J., Su, H., Zorn, S. R., Artaxo, P., and Andreae, M. O.: Rainforest aerosols as biogenic nuclei of clouds and precipitation in the Amazon, Science, 329, 1513-1516, 10.1126/science.1191056, 2010.

Prenni, A. J., Petters, M. D., Kreidenweis, S. M., Heald, C. L., Martin, S. T., Artaxo, P., Garland, R. M., Wollny, A. G., and Poschl, U.: Relative roles of biogenic emissions and Saharan dust as ice nuclei in the Amazon basin, Nature Geoscience, 2, 401-404, Doi 10.1038/Ngeo517, 2009.

Roldin, P., Nilsson, E., Swietlicki, E., Massling, A., and Zhou, J.: *Lund SMPS User's manual*, EUCAARI Brazil Version, 2008.

Shilling, J. E., Chen, Q., King, S. M., Rosenoern, T., Kroll, J. H., Worsnop, D. R., DeCarlo, P. F., Aiken, A. C., Sueper, D., Jimenez, J. L., and Martin, S. T.: Loading-dependent elemental composition of α-pinene SOA particles, Atmos. Chem. Phys., 9, 771-782, 10.5194/acp-9-771-2009, 2009.

Surratt, J. D., Gomez-Gonzalez, Y., Chan, A. W. H., Vermeylen, R., Shahgholi, M., Kleindienst, T. E., Edney, E. O., Offenberg, J. H., Lewandowski, M., Jaoui, M., Maenhaut, W., Claeys, M., Flagan, R. C., and Seinfeld, J. H.: Organosulfate formation in biogenic secondary organic aerosol, J. Phys. Chem. A, 112, 8345-8378, 10.1021/jp802310p, 2008.

Ulbrich, I. M., Canagaratna, M. R., Zhang, Q., Worsnop, D. R., and Jimenez, J. L.: Interpretation of organic components from Positive Matrix Factorization of aerosol mass spectrometric data, Atmos. Chem. Phys., 9, 2891-2918, 2009.

Table S1. Summary of the regression coefficients *m* of instrument comparisons. Expected *m* values are shown in parentheses. These values are estimated on the basis of the diameter domain of the various instruments and an assumed AMS collection efficiency of 1.0, in conjunction with typical mass distributions obtained by MOUDI measurements during the wet season in the Amazon basin (Martin et al., 2010; Pöschl et al., 2010).

	Volume concentration	Number concentration	Sulfate mass concentration	Particle mass concentration	Light scattering at 550 nm
	SMPS	CPC	Filter-based	Filter-based	Nephelometer
AMS	1.24 (1.0)	-	0.90 (1.0)	0.65 (0.7)	0.62 (< 1.0)
SMPS	-	0.59 (< 1.0)	-	-	

Table S2. Summary of the particle mass concentration (μg m^{-3}, STP) measured by the stacked filter units on the 10-m inlet (SFU), by the total-particle filter on the 38-m turbulent inlet (TPF), and by the AMS during AMAZE-08.

Sampling Periods (MM/DD/YY)	SFU: PM_2	TPF: PM_3	AMS: NR-PM_1	AMS/SFU	AMS/TPF
02/10/08 – 02/14/08	2.51	n.a.	1.75	0.70	n.a.
02/14/08 – 02/16/08	1.41	1.30	1.37	0.97	0.87
02/16/08 – 02/19/08	0.87		0.89	1.02	
02/19/08 – 02/22/08	1.14	1.48	0.85	0.75	0.57
02/22/08 – 02/26/08	2.44		0.85	0.35	
02/26/08 – 02/29/08	3.20	2.86	0.96	0.30	0.33
02/29/08 – 03/04/08	3.38		0.99	0.29	
03/04/08 – 03/08/08	1.02	1.02	0.73	0.72	0.72
03/08/08 – 03/12/08	1.01	1.09	0.74	0.73	0.68
Average	**1.89**	**1.55**	**1.02**	**0.65**	**0.63**

List of Figures

periods as the AMS mass-diameter distributions. Valued in all panels are normalized to STP.

Figure S7. Example of the mass-diameter distribution measured by the AMS compared to that derived from the SMPS measurements. The effective particle density ρ_{eff} is determined by the mode diameters. The SMPS mass-diameter distributions were derived by multiplying the SMPS volume-diameter distributions by $\rho_{eff.}$ Data were sampled on March 11, 2008.

Figure S8. (**a**) Time series of the particle volume concentrations obtained by the AMS and the SMPS measurements. (**b**) The ratio of the particle volume concentrations derived from the AMS measurements to the PM_7 light scattering coefficients measured by the nephelometer at 550 nm. The AMS data were averaged to the nephelometer timebase. Gray areas represent the periods that were influenced by the generator exhaust plumes.

~~**Figure S8.** Time series of the relative intensity of *m/z* 60 in the organic mass spectra. The peak at *m/z* 60 is a fragment of levoglucosan and related species and can serve as a marker of biomass burning. The red line represents the threshold value of 0.35% that corresponds to natural background (Docherty et al., 2008).~~

~~**Figure S9.** Mass spectrum of OOA-3 compared to the synthetic mass spectrum obtained from a linear combination of the mass spectra (cf. Fig. 6) of laboratory-generated biogenic SOM (30% α-pinene SOM, 20% β-caryophylene SOM, and 50% isoprene SOM).~~

Figure S9. Time series of the model residuals e_{ij} for the PMF analysis with *FPEAK* of zero. Terms include factor *j*, time *i*, and error σ.

Figure S10. Pearson's R (black dots) for the correlations between the time series and the mass

spectra of any two factors (tagged as x_y) for the PMF solutions for a preset of different number of factors (*p*).

Figure S11. (**a**) The mass spectra of the statistical factors identified by the PMF analysis for Ffour-factor solutionsolutions and ns for selected *FPEAK* (f_{peak}) values. (**b**) Time series of mass concentrations for the statistical factors.

Figure S12. The mass spectrum of HOA with from the bootstrapping analysis of four-factor PMF solutions. Average (black) with 1-σ error bars (red) are shown.

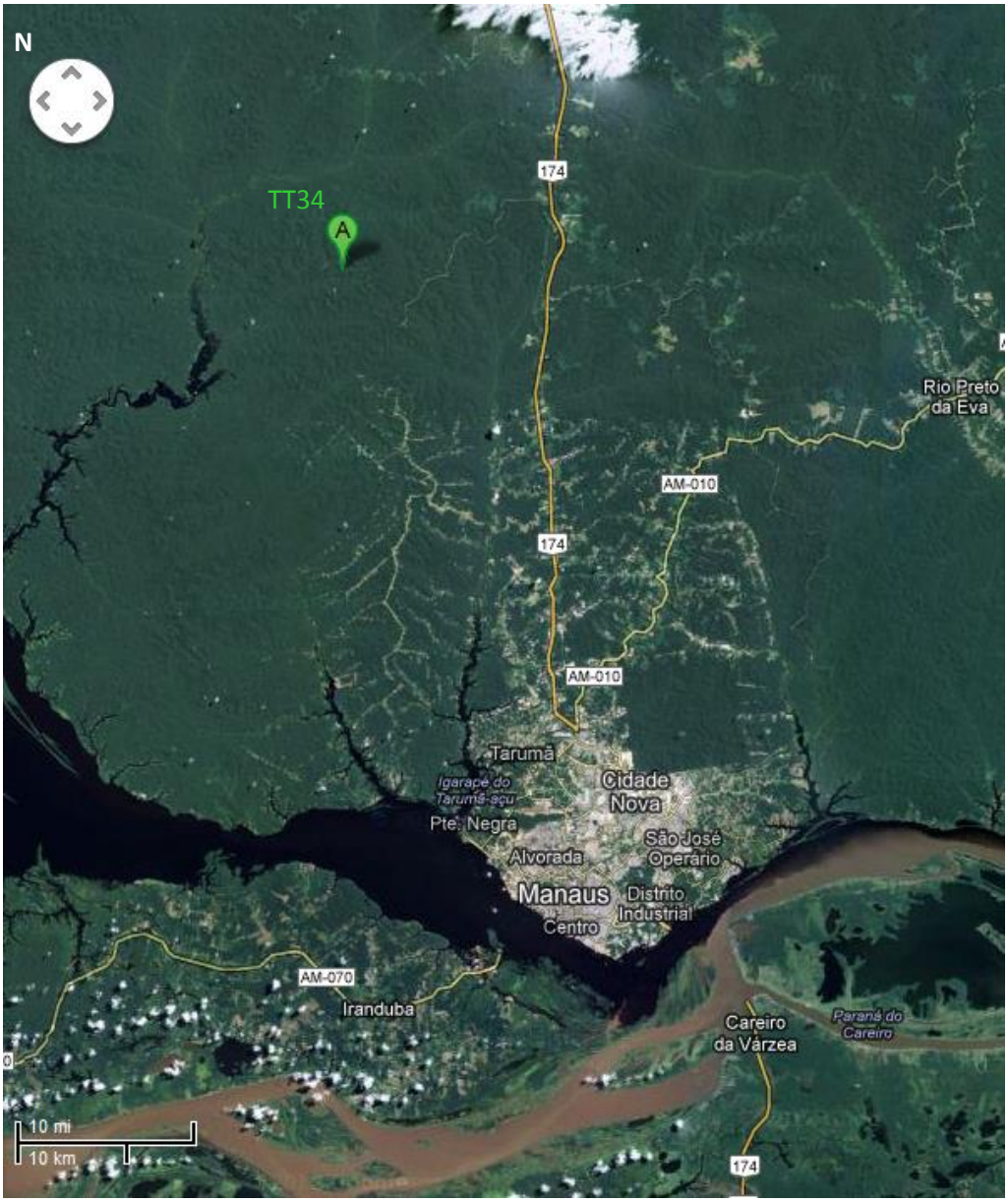
N
TT34
A
174
Rio Preto
da Eva
AM-010
174
AM-010
Tarumã
Igarapé do
Tarumã-açu
Cidade
Nova
Pte. Negra
São José
Operário
Alvorada
Manaus
Distrito
Industrial
Centro
AM-070
Iranduba
Careiro
da Várzea
Paraná do
Careiro
10 mi
10 km
174

Figure S1

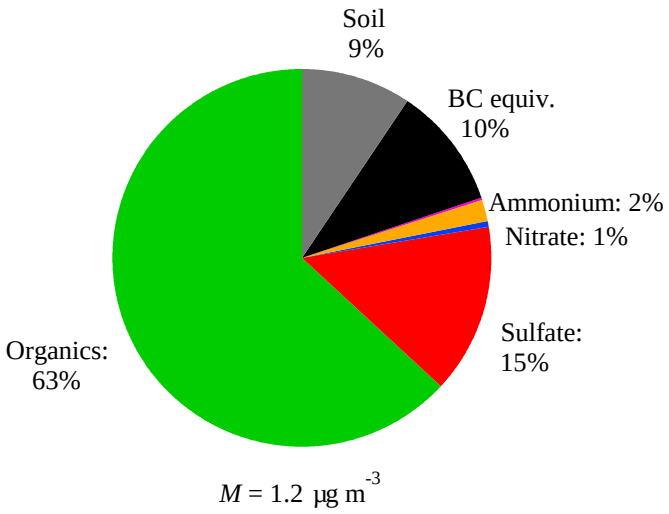
Soil
9%
BC equiv.
10%
Ammonium: 2%
Nitrate: 1%
Sulfate:
15%
Organics:
63%
M = 1.2 µg m-3

Figure S2

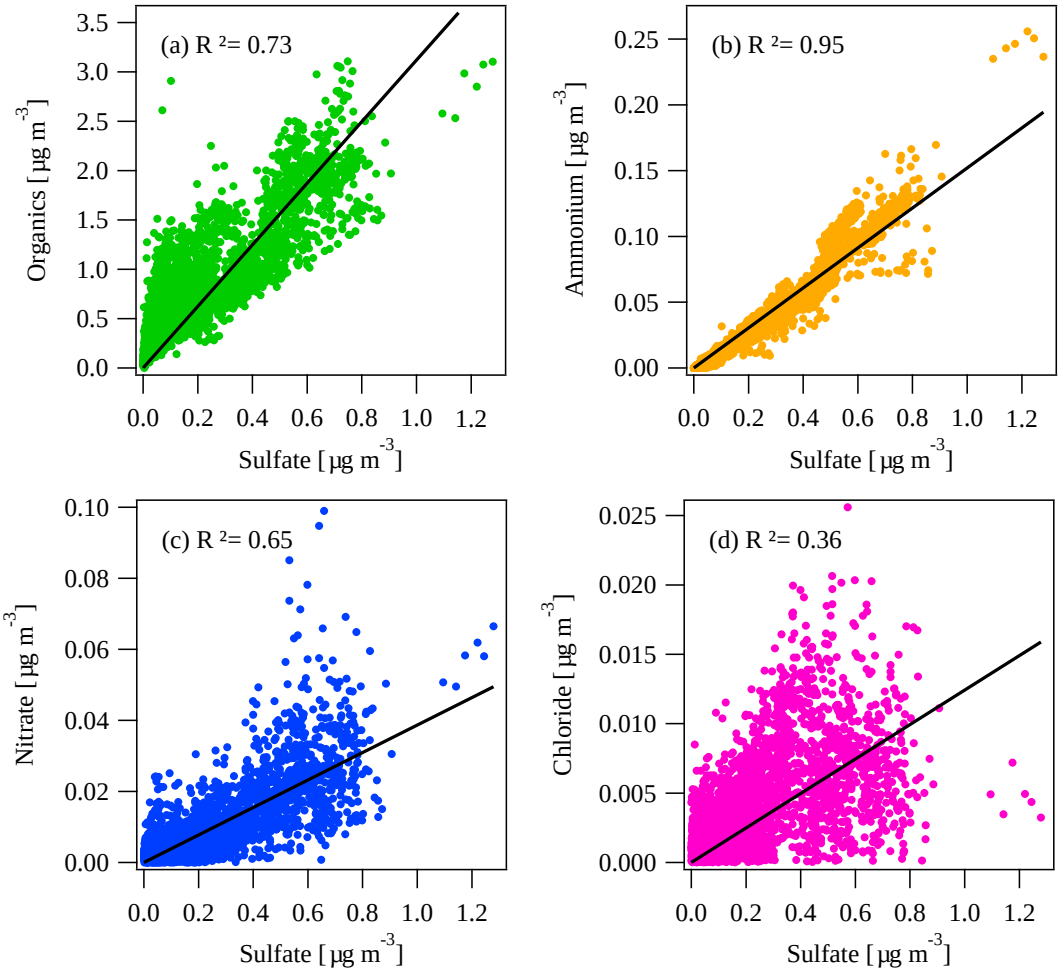
(a) R ²= 0.73
Organics [µg m-3]
Sulfate [µg m-3]
(b) R ²= 0.95
Ammonium [µg m-3]
Sulfate [µg m-3]
(c) R ²= 0.65
Nitrate [µg m-3]
Sulfate [µg m-3]
(d) R ²= 0.36
Chloride [µg m-3]
Sulfate [µg m-3]

Figure S3

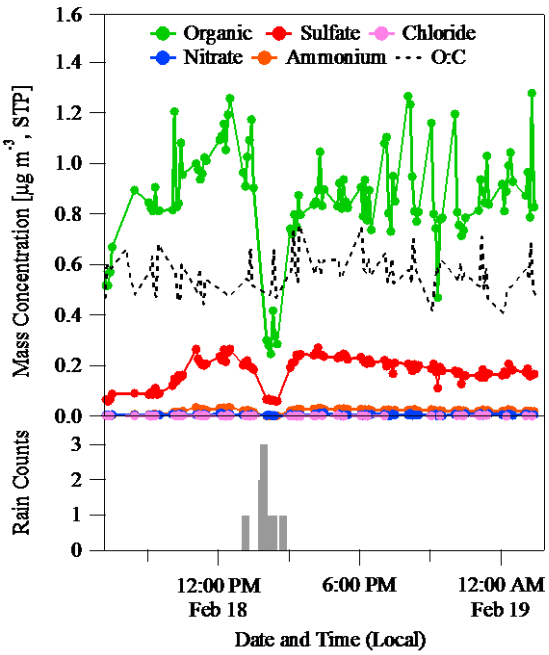
Organic
Sulfate
Chloride
Nitrate
Ammonium
O:C
Mass Concentration [µg m-3, STP]
1.6
1.4
1.2
1.0
0.8
0.6
0.4
0.2
0.0
Rain Counts
3
2
1
0
12:00 PM
Feb 18
6:00 PM
12:00 AM
Feb 19
Date and Time (Local)

Figure S4

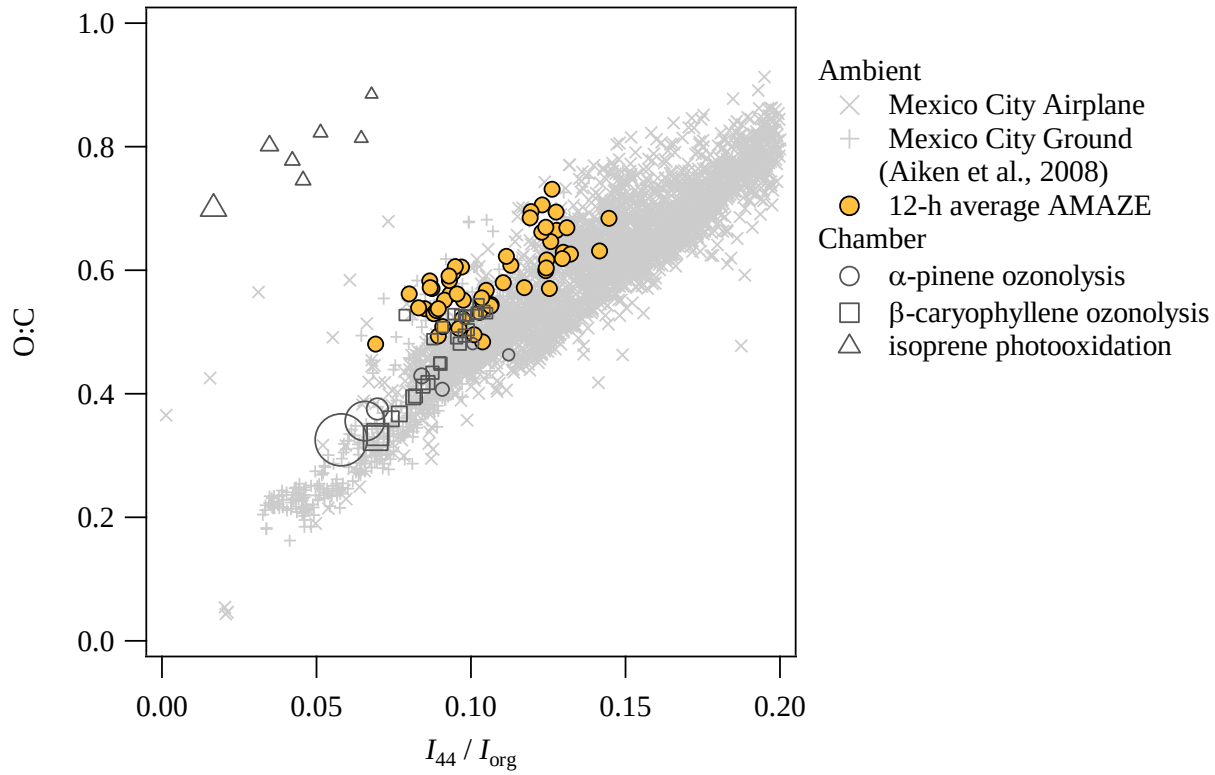
1.0
0.8
0.6
0.4
0.2
0.0
O:C
0.00
0.05
0.10
0.15
0.20
I_{44} / I_{org}
Ambient
Mexico City Airplane
Mexico City Ground
(Aiken et al., 2008)
12-h average AMAZE
Chamber
α-pinene ozonolysis
β-caryophyllene ozonolysis
isoprene photooxidation

Figure S5

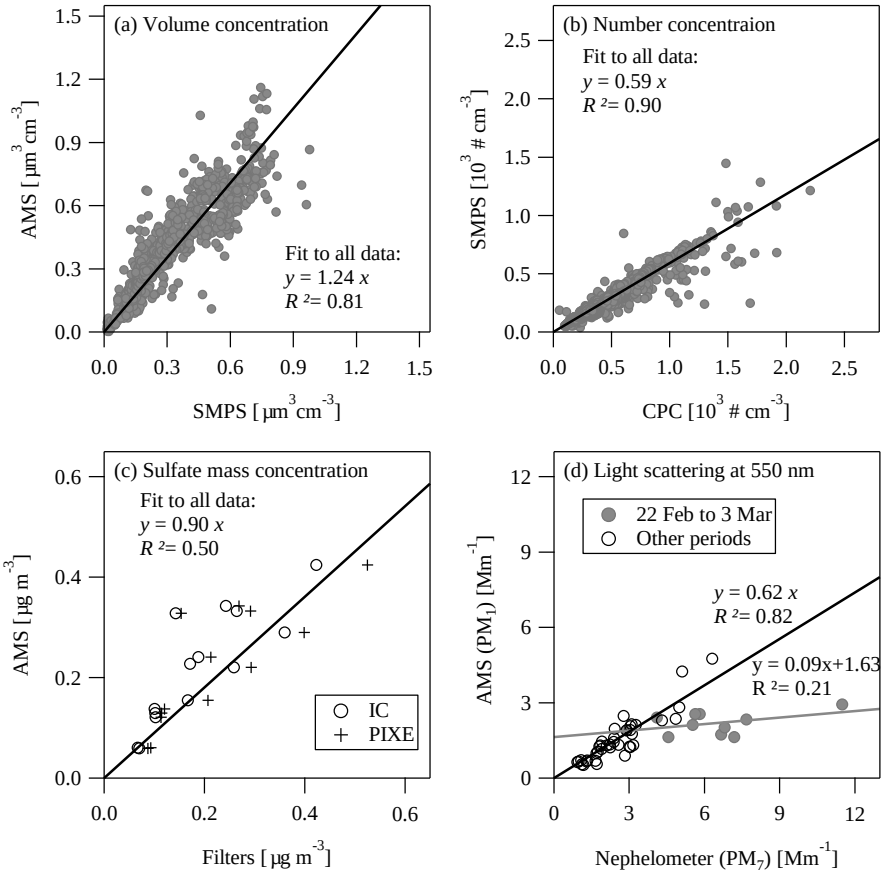
(a) Volume concentration
Fit to all data:
y = 1.24 x
R ²= 0.81
AMS [µm ³ cm ⁻³]
SMPS [µm³ cm⁻³]
(b) Number concentraion
Fit to all data:
y = 0.59 x
R ²= 0.90
SMPS [10³ # cm⁻³]
CPC [10³ # cm⁻³]
(c) Sulfate mass concentration
Fit to all data:
y = 0.90 x
R ²= 0.50
IC
PIXE
AMS [µg m⁻³]
Filters [µg m⁻³]
(d) Light scattering at 550 nm
22 Feb to 3 Mar
Other periods
y = 0.62 x
R ²= 0.82
y = 0.09x+1.63
R ²= 0.21
AMS (PM1) [Mm⁻¹]
Nephelometer (PM7) [Mm⁻¹]

Figure S6

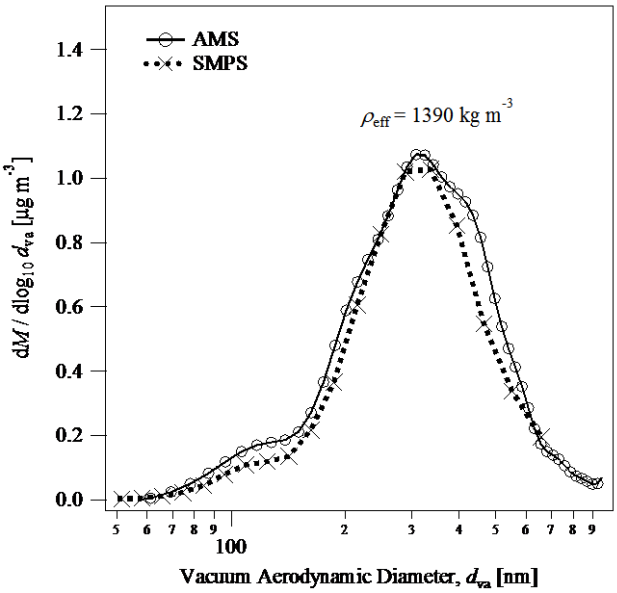
AMS
SMPS
ρ_{eff} = 1390 kg m^{-3}
dM / dlog$_{10}$ d_{va} [µg m^{-3}]
1.4
1.2
1.0
0.8
0.6
0.4
0.2
0.0
5 6 7 8 9
100
2 3 4 5 6 7 8 9
Vacuum Aerodynamic Diameter, d_{va} [nm]

Figure S7

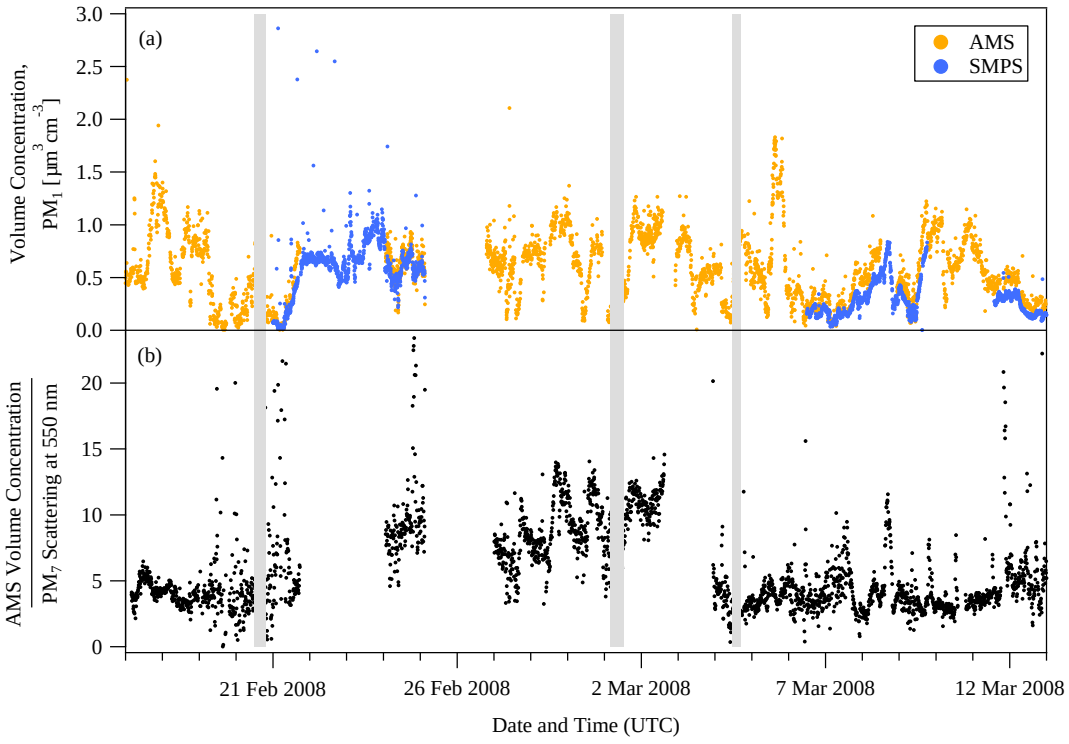
(a)
AMS
SMPS
Volume Concentration, PM1 [µm3 cm-3]
3.0
2.5
2.0
1.5
1.0
0.5
0.0
(b)
AMS Volume Concentration / PM7 Scattering at 550 nm
20
15
10
5
0
21 Feb 2008
26 Feb 2008
2 Mar 2008
7 Mar 2008
12 Mar 2008
Date and Time (UTC)

Figure S8

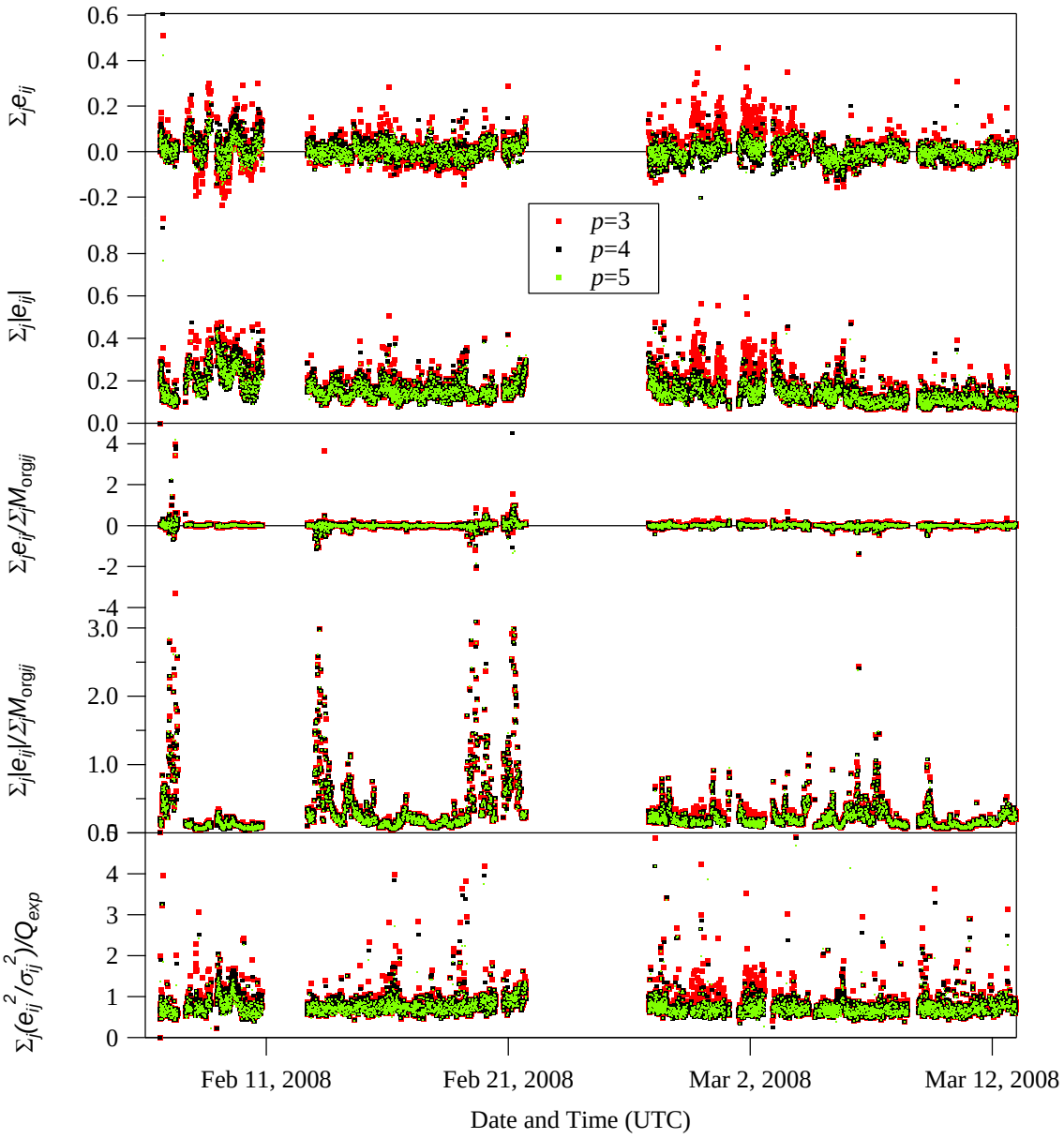
$\Sigma_j e_{ij}$
$\Sigma_j |e_{ij}|$
$\Sigma_j e_{ij} / \Sigma_j M_{orgij}$
$\Sigma_j |e_{ij}| / \Sigma_j M_{orgij}$
$\Sigma_j (e_{ij}^2 / \sigma_{ij}^2) / Q_{exp}$
p=3
p=4
p=5
Feb 11, 2008
Feb 21, 2008
Mar 2, 2008
Mar 12, 2008
Date and Time (UTC)

Figure S9

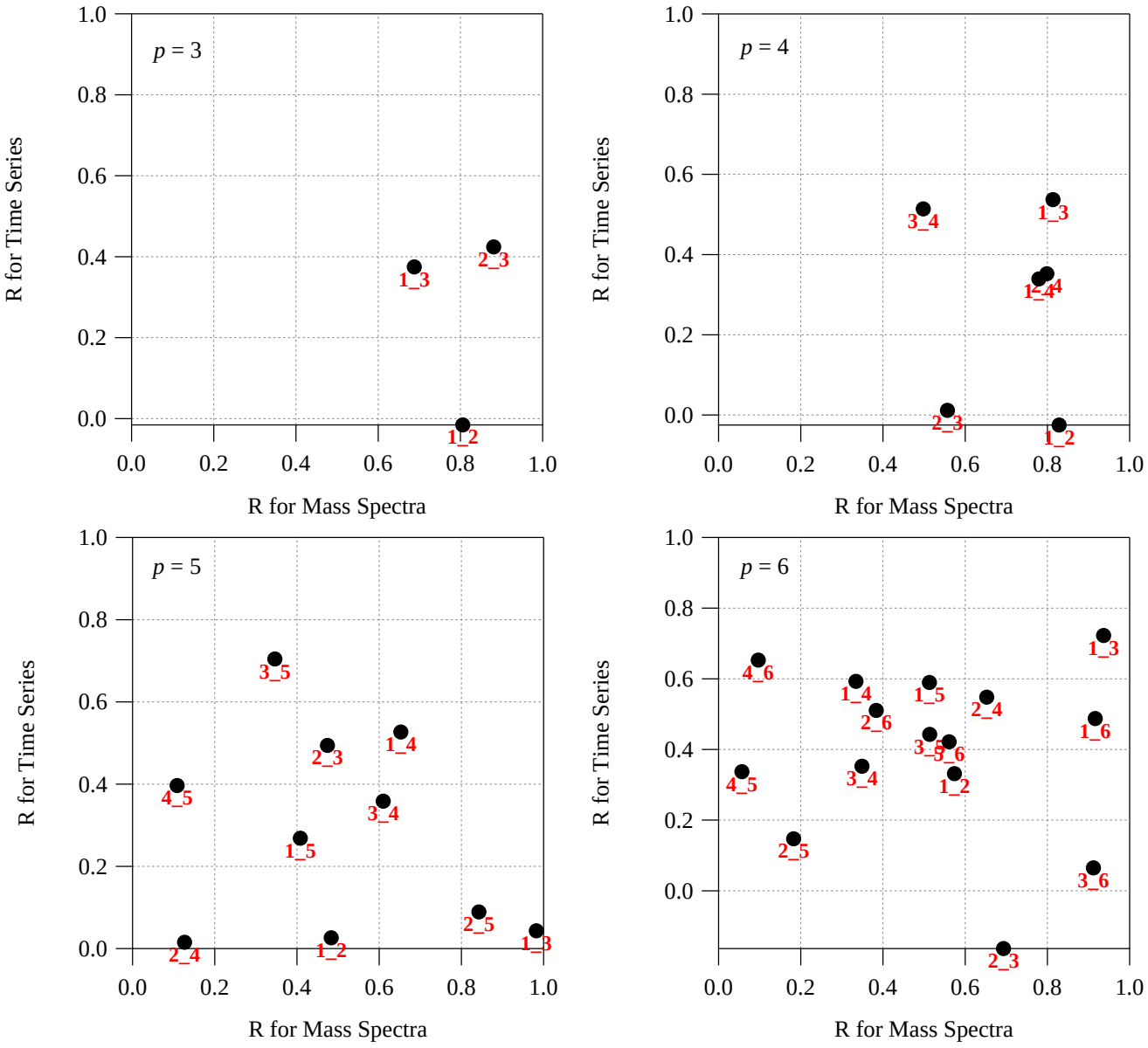
p = 3
1_3
2_3
1_2
p = 4
3_4
1_3
1_4
2_3
1_2
p = 5
3_5
2_3
1_4
4_5
3_4
1_5
2_5
2_4
1_2
1_3
p = 6
4_6
1_4
1_5
2_4
1_3
2_6
3_5
3_6
1_6
4_5
3_4
1_2
2_5
3_6
2_3
R for Time Series
R for Mass Spectra
0.0
0.2
0.4
0.6
0.8
1.0

Figure S10

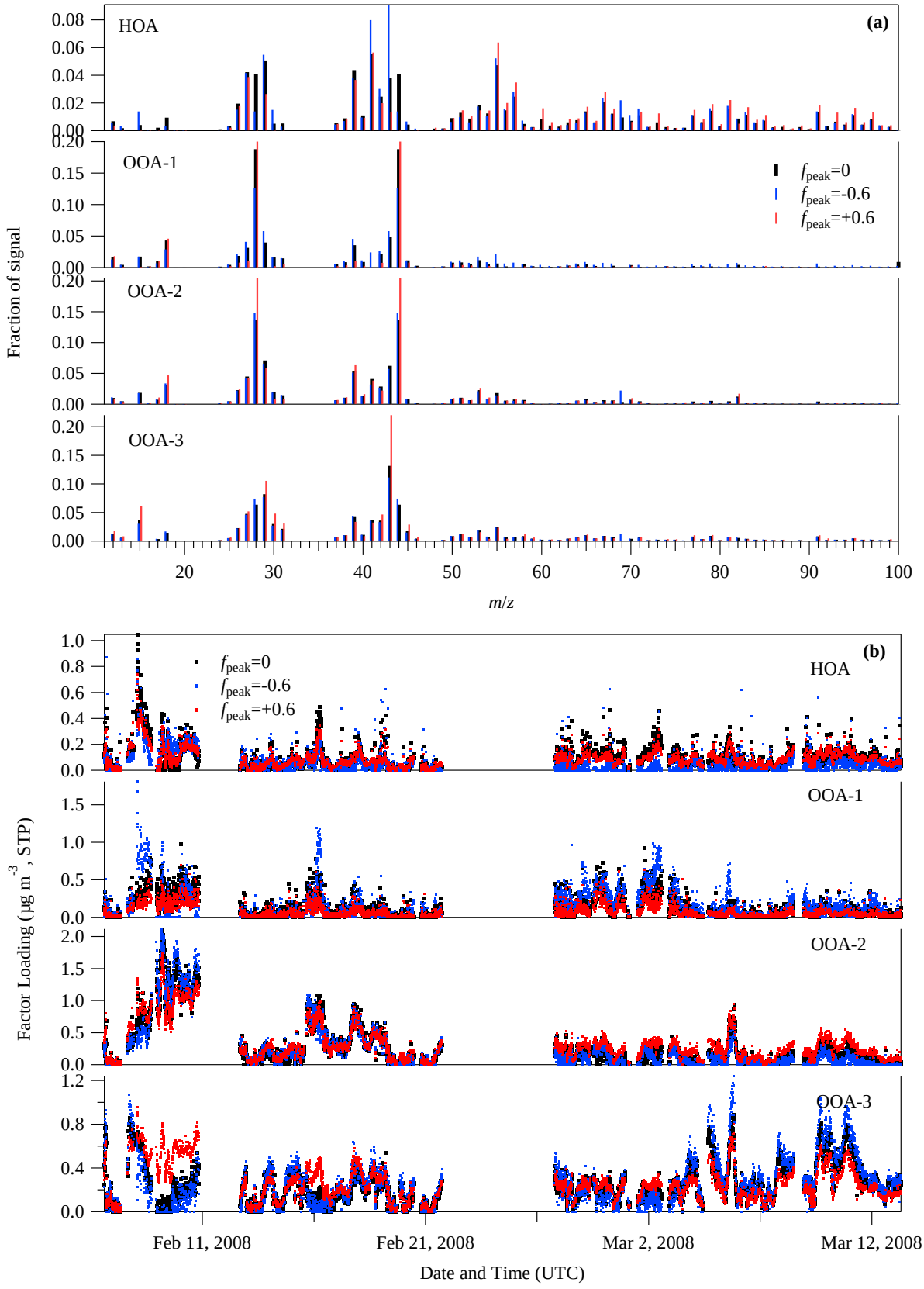
(a)
HOA
OOA-1
OOA-2
OOA-3
f_{peak}=0
f_{peak}=-0.6
f_{peak}=+0.6
Fraction of signal
m/z
(b)
HOA
OOA-1
OOA-2
OOA-3
Factor Loading (μg m^{-3}, STP)
Feb 11, 2008
Feb 21, 2008
Mar 2, 2008
Mar 12, 2008
Date and Time (UTC)

Figure S11

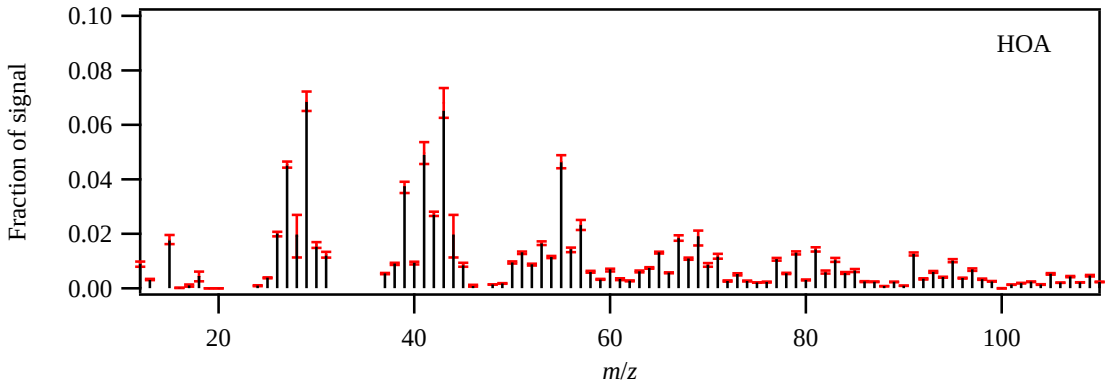
HOA
Fraction of signal
0.10
0.08
0.06
0.04
0.02
0.00
20
40
60
80
100
m/z

Figure S12